catalysts

MDPI

Review

Investigation of Electrocatalytic Applications of Various Advanced Nanostructured Alloys—An Overview

Shashanka Rajendrachari [1,*], Gireesha R. Chalageri [2], Rayappa Shrinivas Mahale [3], Emre Altas [4], Yashwant Chapke [3] and Vinayak Adimule [5]

[1] Department of Basic Sciences, School of Sciences and Humanities, SR University, Warangal 506371, India
[2] School of Mechanical Engineering, KLE Technological University, Hubballi 580031, India; gireesha@kletech.ac.in
[3] Department of Automation and Robotics, JSPMs Rajarshi Shahu College of Engineering, Pune 411033, India; rayappamahale@gmail.com (R.S.M.); yashchapke@gmail.com (Y.C.)
[4] Department of Mechanical Engineering, Faculty of Engineering, Architecture and Design, Bartın University, Bartin 74110, Turkey; emrealtas@bartin.edu.tr
[5] Department of Chemistry, Angadi Institute of Technology and Management (AITM), Savagaon Road, Belagavi 590009, India; chemistry@aitmbgm.ac.in
* Correspondence: shashankaic@gmail.com

Abstract: Cyclic voltammetry (CV) is one of the advanced techniques used to determine various bioactive molecules, organic dyes, pesticides, veterinary drugs, heavy metals, toxic chemicals, etc. To determine all the above analytes, one needs an electrocatalyst for their electrochemical redox reaction. Many researchers have reported the use of metal nanomaterials, metal oxide nanomaterials, metal–organic frameworks, surfactants, polymers, etc., as modifiers in carbon paste electrodes to enhance their current response, stability, sensitivity, and repeatability. But some of the emerging, cost-effective, and highly efficient electrocatalysts are advanced nanostructured alloy powders. These advanced alloys are used as a modifier to determine various bioactive analytes. These alloy-modified carbon paste electrodes (MCPEs) show excellent selectivity, sensitivity, and stability due to their extraordinary electrochemical properties, as the compositional elements of most of the alloys belong to d-block elements in the periodic table, and these transition elements are famous for their brilliant electrocatalytic properties. The present review article mainly focuses on the determination of dopamine, AA (AA), uric acid, methylene blue, methyl orange, Rhodamine B, and the L-Tyrosine amino acid by various alloys like stainless steel, high-entropy alloys, and shape-memory alloys and how these alloys could change the perception of metallurgists and electrochemists in the future. These alloys could be potential candidates for the development of various electrochemical sensors because of their high porosity and surface areas.

Keywords: mechanical alloying; nanostructured alloys; electrocatalysts; modifiers; carbon paste electrode

check for updates

Academic Editor: Vincenzo Baglio

Received: 28 January 2025
Revised: 21 February 2025
Accepted: 21 February 2025
Published: 7 March 2025

Citation: Rajendrachari, S.; Chalageri, G.R.; Mahale, R.S.; Altas, E.; Chapke, Y.; Adimule, V. Investigation of Electrocatalytic Applications of Various Advanced Nanostructured Alloys—An Overview. *Catalysts* **2025**, *15*, 259. https://doi.org/10.3390/catal15030259

Copyright: © 2025 by the authors. Licensee MDPI, Basel, Switzerland. This article is an open access article distributed under the terms and conditions of the Creative Commons Attribution (CC BY) license (https://creativecommons.org/licenses/by/4.0/).

1. Introduction

Numerous medicinal and environmental applications depend on the quick and accurate detection of bioactive compounds. Conventional biomolecule detection techniques like spectroscopy and chromatography are frequently costly and time-consuming and necessitate intricate sample preparation [1,2]. We are in great need of analytical instruments that are highly sensitive, selective, stable, and robust in determining various bioactive compounds individually or simultaneously [3]. In analytical chemistry, medicine, and

environmental monitoring, the creation of electrochemical sensors for the detection of bioactive compounds has grown in importance. High sensitivity, selectivity, and affordability, as well as the capacity for quick real-time analysis, are just a few benefits that these sensors provide [4]. Nowadays, electrochemical techniques like CV, electrochemical impedance spectroscopy, alternating current voltammetry, differential pulse voltammetry, photo-induced electrochemiluminescence, and electrochemiluminescence are highly efficient and effective techniques for determining bioactive compounds, organic dyes, surfactants, toxic chemicals, etc. [5]. Among these, CV is one of the popular electrochemical techniques performed by cycling the potential of working electrodes between two chosen values to determine the resultant current [6]. CV is a strong, sensitive, and adaptable technique for examining bioactive compounds in both research and clinical settings [7]. In domains including drug development, biomarker detection, and bioanalytical chemistry, it is essential to figure out their electrochemical characteristics, interactions, stability, and possible therapeutic uses. CV provides detailed information about the redox behavior of bioactive compounds, as well as their electrochemical reactivity, electron transfer kinetics, reaction mechanism, and quantitative and qualitative analysis [8].

Even though electrochemical sensors exhibit potential advantages, they still exhibit a few limitations in terms of selectivity, stability, sensitivity, and repeatability. To overcome these limitations, many researchers have used carbon paste electrodes (CPEs), which are stable, selective, economic, and consistent in detecting various bioactive compounds. Among the several electrochemical sensor platforms, carbon paste electrodes (CPEs) have widely attracted researchers due to their versatile properties, ease of preparation, and low manufacturing costs. Many researchers have used carbon paste electrodes (CPEs) to determine various bio-analytes using the CV technique [9–11], and it has been proven that these electrodes are highly stable, repeatable, sensible, and selective in nature. Further, these electrode properties can be improved by modifying CPEs with nanomaterials. These nanomaterials exhibit excellent values for surface area and surface energy, which can further improve the electrocatalytic properties of the electrode [12,13]. Many researchers have used various metal nanoparticles, metal oxide nanoparticles, and carbon-nanomaterial-modified CPEs [14–20], but very few researchers have reported the use of nanostructured alloys as modifiers.

The present review hypothesizes that the idea of adding nanostructured alloys like stainless steel, HEA, and shape-memory alloys into CPEs during the determination of various analytes will improve the sensitivity, selectivity, and stability of electrochemical sensors to a greater extent [21–24]. This could also overcome CPEs' limitations, like their poor conductivity, low stability, and sensitivity at low concentrations of the analyte, and improve their detection limits and quantification limits. These changes provide the sensors with the ability to identify a variety of bioactive compounds at low concentrations, which is crucial for tracking the levels of therapeutic drugs for the early diagnosis of illnesses, determining various toxic dyes present in water, etc. The main objective of the present review is to study the effects of modifiers, like nanostructured alloys on the electrochemical detection of various bioactive compounds, and also how they affect the sensitivity, selectivity, and stability of the electrodes at lower concentrations of the analyte.

2. Advantages of Using Nanostructured Alloys as Modifiers

One of the main advantages of using alloys as modifiers is their extraordinary stability; most alloys remain stable and do not undergo any undesirable electrochemical reactions, even with a wide range of potentials [25,26]. This will prevent the alloys from undergoing decomposition at higher operating voltages. One more characteristic of alloys is their electrode potential; the different elements present in an alloy can impart their electrode

potential, resulting in a characteristic electrode potential that is obtained from all the elements present in an alloy. This electrode potential plays an important role in determining the electrocatalytic properties of alloys during the electrochemical redox reactions of the analytes [27–30]. In this review article, we reported the nanostructured alloys prepared from mechanical alloying. This method increases the surface area, and surface roughness of the alloys by refining their structures, and also improves their porosity ratios, thereby improving their electrocatalytic properties. The presence of different metals in an alloy results in heterogeneous surface characteristics, which have a strong influence on the electrochemical properties of the alloys [31–33]. On the other hand, surface roughness further improves the electrocatalytic properties of the alloy by creating reactive sites for the mobility of electrons.

3. Fabrication of Nanostructured Alloys by Ball-Milling Method

Recently, the ball-milling method has emerged as a well-established technique for fabricating nanostructured alloys, especially for producing fine powders of metallic alloys with improved qualities including strength, hardness, and wear resistance [34–36]. To create nano-sized grain formations, powders of various metals or elements are combined and processed under high energy conditions in a mechanical alloying process called ball milling. Figure 1 depicts the planetary ball mill present at Bartin University, Turkey.



Figure 1. Retsch PM 100 planetary ball mill present in Bartin University, Turkey.

Ball milling is a technique composed of rotating cylindrical chambers loaded with steel or ceramic balls. The fundamental process involves adding the elemental powders to the grinding media at specific ball-to-powder weight ratios. The balls and powder collide as the mill turns, breaking up and reshaping the particles to produce finer powders. The impact and friction between the grinding balls and the particles provide the mechanical energy necessary for the ball-milling process [37]. A refined structure is produced as the particles are crushed, deformed, and welded by the balls as they tumble and revolve in the mill. As a result, nanoparticles are created, and solid-state processes can be triggered to create alloys [38,39]. For further details about ball milling, milling conditions, and how to prepare nanostructured alloys, refer to the published articles of the author of this review, Shashanka et al. [31,32,40–42]. The main advantages of using the mechanical alloying method are because of its low cost, scalability, versatility, improved properties,

uniform homogeneity, control over the method, etc. Therefore, many researchers use mechanical alloying methods to prepare various advanced alloys. While preparing alloys by ball-milling method, one must take care of contamination, agglomeration, improper distribution of alloy, chances of wearing of machines, etc. In the present review article, we have discussed the electrocatalytic properties of DS, ferritic stainless steel, high-entropy alloys, and shape-memory alloys prepared by the ball-milling method.

4. Preparation of Nanostructured-Alloys-Modified Carbon Paste Electrodes (NsA-MCPE)

To prepare CPEs, we need graphite powder and a binder like paraffin oil or silicone oil. The proportion of binder to graphite powder is crucial [43,44]. The standard ratios of 70–80% graphite powder by weight and 20–30% binder, such as silicone oil, are mixed well in mortar and pestle for approximately 30 min [45,46]. Depending on the particular requirements of the experiment and the characteristics of the graphite powder, we can modify this ratio. To create a homogenous mixture, thoroughly mix the graphite powder and the binder material [47,48]. The carbon paste should resemble thick toothpaste in consistency and be uniformly smooth. Later, fill the carbon paste to the cavity present in the specially designed electrode, which acts as the working electrode. Make sure to fill it evenly to avoid air bubbles and ensure the paste is tightly packed. Leave a small part of the electrode body free of paste to attach the electrical contact. Carbon paste is packed properly and uniformly to avoid any formation of air bubbles in the electrode. To obtain a homogeneous smooth surface for electrochemical measurements, gently press the carbon paste electrode against a clean piece of paper towel or a level surface. To the surface of the CPE, attach a suitable conductive wire like copper for the electrical contact for the electrode. To avoid unwanted side reactions, make sure the copper wire is properly in contact with the carbon paste without touching the electrode's exposed surface [49,50]. Sometimes, curing of the electrode may require that, depending upon the type of binder used. Curing is a process of heating the electrode at a very low temperature to solidify the binder used to prepare the CPE; this will impart mechanical strength to the electrode. If we use mineral oil as a binder, then the CPE requires curing, and if we use silicone oil as a binder, then curing is not required. Curing of electrodes is required only when we use low-viscous binders to prepare the CPEs. After curing, we need to polish the surface of the electrode to make it smooth and uniform. On the other hand, NsA-MCPE is prepared by mixing different concentrations of the modifier (nanostructured alloys) in a CPE composition and grinding them with a mortar and pestle for approximately 30 min and follow the same steps as discussed above to prepare CPEs. Figure 2 depicts the CPE preparation process.

It is very important to pre-condition the electrode by applying multiple potential cycles in the electrochemical solution under study using cyclic voltammetry. This can help the electrode to perform consistently throughout measurements by eliminating contaminants or irregular side reactions because of them. Now, the electrode is ready to use for the electrochemical determination of various bioactive compounds by cyclic voltammetric method and placed in an analyte solution, along with a reference electrode and platinum wire counter electrode [51–53].

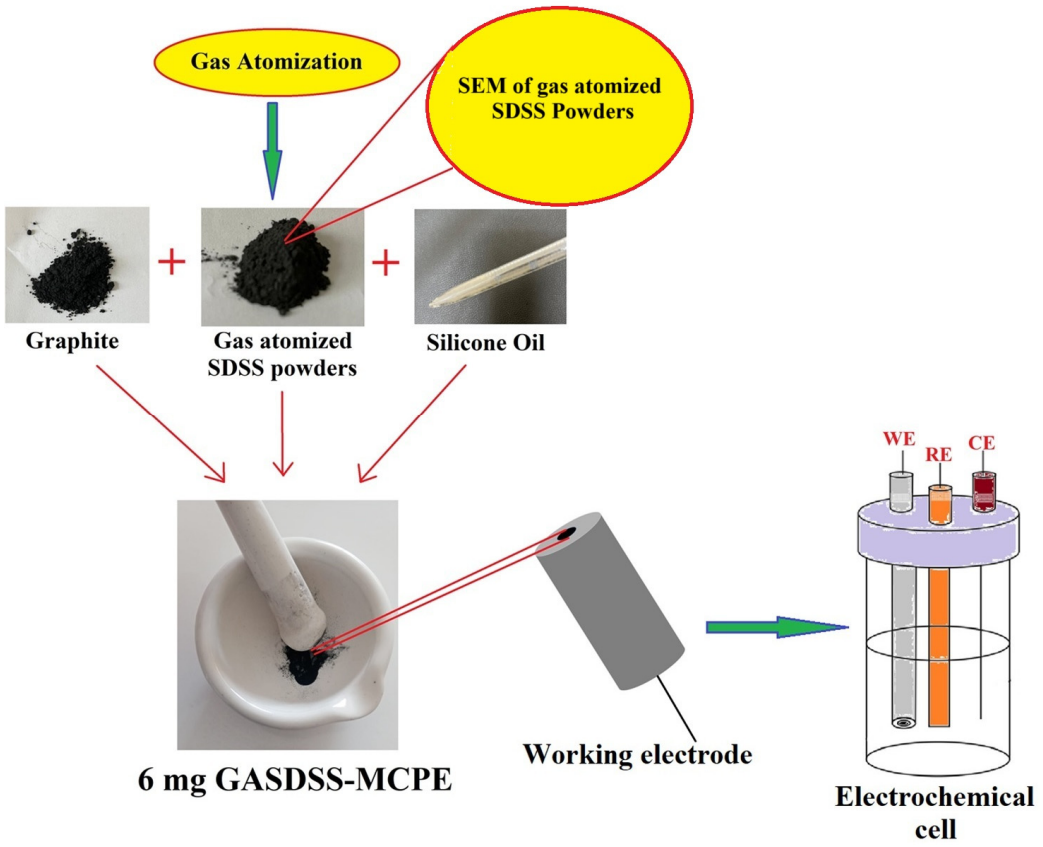


Figure 2. Preparation of CPE [28].

5. Duplex Stainless Steel-Modified Carbon Paste Electrode (DS-MCPE)

5.1. Introduction to Duplex Stainless Steel (DS)

DS is a popular grade of stainless steel, made up of nearly equal amounts of non-magnetic ferrite and magnetic austenite phases [54–56]. DS is appropriate for demanding applications requiring high strength, exceptional corrosion resistance, electrochemical properties, good weldability, high toughness, and enhanced fatigue resistance due to their dual-phase structure [57–59]. The marine, oil and gas, paper and pulp, chemical processing, and construction industries are among those that employ DS because of its exceptional strength, corrosion resistance, and affordability [60,61]. Recent applications of DSs are used as an electrocatalyst for various electrochemical applications [26–28].

5.2. Electrochemical Determination of Dopamine

Dopamine functions as a chemical messenger known as a neurotransmitter, which transmits messages to the brain through the central nervous system [62]. It is essential for numerous bodily processes, such as motivation, pleasure, happiness, mobility, and emotional response management. The ventral tegmental area (VTA) and the substantia nigra present in the brain manufacture dopamine. It is a component of the dopaminergic system, which affects mood, behavior, and even judgment [63,64]. Tyrosine, an amino acid, is the precursor for dopamine. It undergoes enzymatic processes to transform into L-DOPA and, subsequently, dopamine. When dopamine is produced, it attaches itself to target neurons' dopamine receptors to affect their activity. Deficiency of dopamine can affect the central nervous system and mental health, increase anxiety and depression, and cause attention deficit hyperactivity disorder (ADHD), Parkinson's disease, compulsive behavior, sleeping disorders, etc. [65–68]. Therefore, we must determine dopamine efficiently and

effectively. The cyclic voltammetric method proved to be one of the best techniques used to determine dopamine. The chemical structure of dopamine is shown in Figure 3.

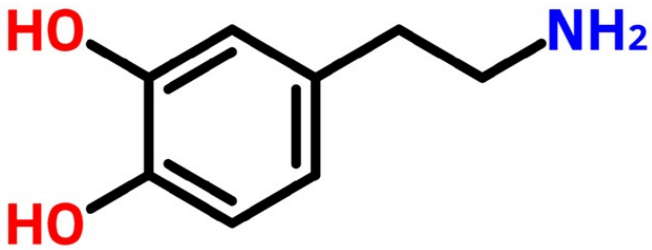


Figure 3. Chemical structure of dopamine [69].

In a reversible electrochemical process, dopamine is reduced and oxidized. Dopamine can usually be reduced back to its original form after being oxidized at the working electrode to produce dopamine quinone. Dopamine undergoes oxidation around +0.2 to +0.6 V to form dopamine quinone and, on the other hand, it will be reduced from dopamine quinone to dopamine at a potential of around +0.1 to +0.3 V. The resultant peak current of the electrochemical redox reaction is proportional to the concentration of dopamine present. The electrochemical determination of dopamine utilizing the DS-MCPE by cyclic voltammetry method was reported by Shashanka et al. [25]. The CV of a bare carbon paste electrode (BCPE) and 4 mg of DS-MCPE in 2 mM of DA at 100 mVs^{-1} and in a pH 7.2 phosphate buffer solution (PBS) is shown in Figure 4a. They have investigated one of the most crucial factors like modifier concentrations to determine the effectiveness of the electrode's performance as a dopamine sensor. To measure dopamine, they have utilized 2, 4, 6, and 8 mg of DS-MCPE; however, 4 mg of DS-MCPE has demonstrated the highest current response compared to the others. To investigate the effects of scan rate, dopamine concentrations, and pH, they utilized 4 mg of DS-MCPE. The corresponding CVs are displayed in Figure 4b, Figure 4c and Figure 4d, respectively.

As the scan rate is increased from 50 to 500 mVs^{-1}, the anodic and cathodic peak currents of dopamine increase during the electrochemical redox reaction due to direct electron transfers between the analyte and the electrode, as illustrated in Figure 4b. The potential difference between the anodic and cathodic peak potentials rises with the scan rate. Similarly, Figure 4c depicts that, as the concentration of dopamine increases from 2 to 3 mM, the anodic peak current (Ipa) also increases from 15.5 to 19 μA. This is because there are more dopamine molecules available at increasing concentrations, which causes Ipa to rise linearly. However, as can be seen in Figure 4d, pH tests suggest that dopamine's anodic peak potential (Epa) drops when the pH rises from 5.7 to 8. This is because protons (H^+) are frequently involved in the oxidation reaction and their concentration decreases as pH rises. This variation in proton concentration alters the electrochemical reaction's equilibrium and influences the voltage at which oxidation takes place. A basic explanation of the relationship between peak potential and pH is given by the Nernst equation; the shift is usually approximately 59 mV per pH unit, depending on the number of protons in the reaction. All these above results prove that DS-MCPE could be a potential candidate to use as an electrocatalyst to determine dopamine electrochemically using cyclic voltammetry.

5.3. Electrochemical Determination of AA

AA is a water-soluble and vital vitamin to human health, also referred to as vitamin C [70]. The molecular formula for this organic compound is $C_6H_8O_6$ and its chemical structure is shown in Figure 5. As a strong antioxidant, AA is essential for many physiological functions, such as collagen formation, bone, cartilage, and tooth maintenance, as well as immune system support [71,72]. Being an antioxidant, AA aids in scavenging free radicals

and shielding the organism from oxidative damage. Vitamin E and other nutrients are also preserved as a result of this antioxidant action. Many fruits and vegetables, including bell peppers, oranges, strawberries, and kiwis, naturally contain AA [73,74]. It must be received through diet or supplements because humans are unable to produce it internally.

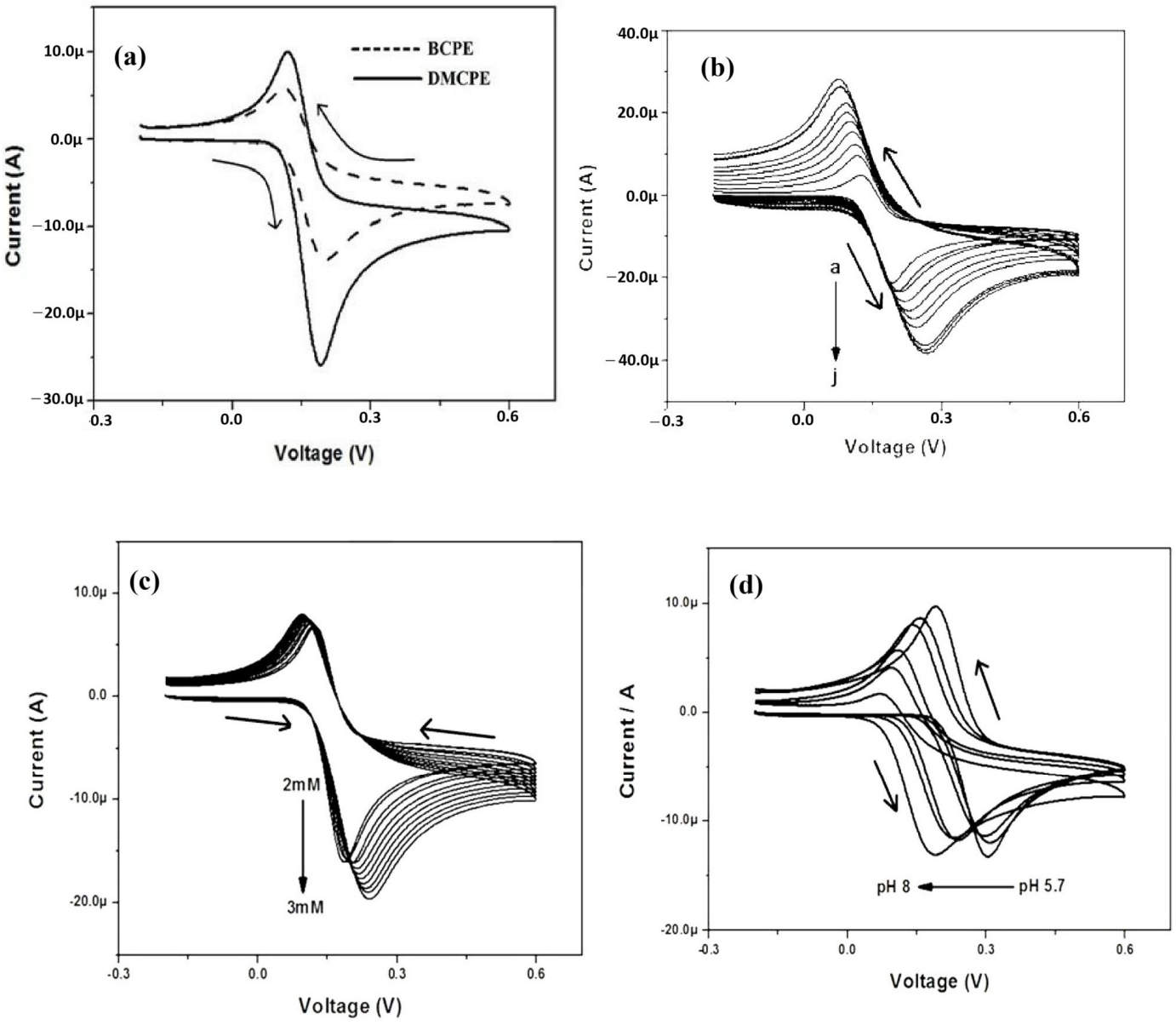


Figure 4. CV of (**a**) BCPE and DS MCPE, (**b**) scan rate investigations at (a = 50, b = 100, …, j = 500 mV/s), (**c**) concentration variation of dopamine, (**d**) pH variation investigation on the redox reaction of dopamine using DS-MCPE [25].

AA is susceptible to air, heat, and light, and when it is exposed to air or UV radiation, it readily breaks down and loses its vitamin function. Because of this, it is frequently kept in cool, dark places and preserved in sealed containers. A typical dietary supplement of AA is used to prevent and cure vitamin C deficiency, which can result in scurvy, and its deficiency can also cause chronic illness, which causes malabsorption of nutrients [75,76]. Since the body cannot generate AA, it must be regularly consumed through diet or supplements to maintain good health [75–77]. Therefore, we need to frequently check for the AA and there are many techniques available to determine it. However, cyclic voltammetry is one of the most accurate ways to identify AA.

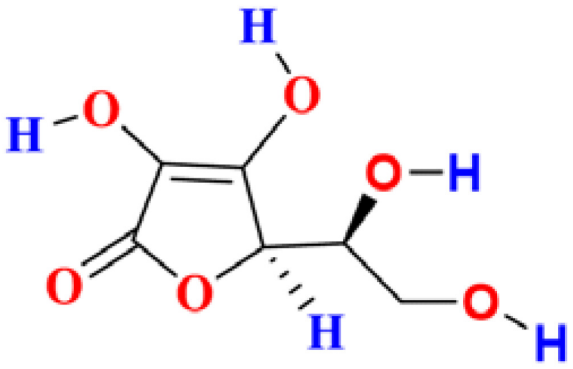


Figure 5. AA structure [77].

The use of mechanically alloyed nanostructured DS powders for electrochemical sensors was reported by Rayappa et al. [26]. The microstructure, lattice spacing, and SAED pattern of mechanically alloyed DS are shown in Figure 6.

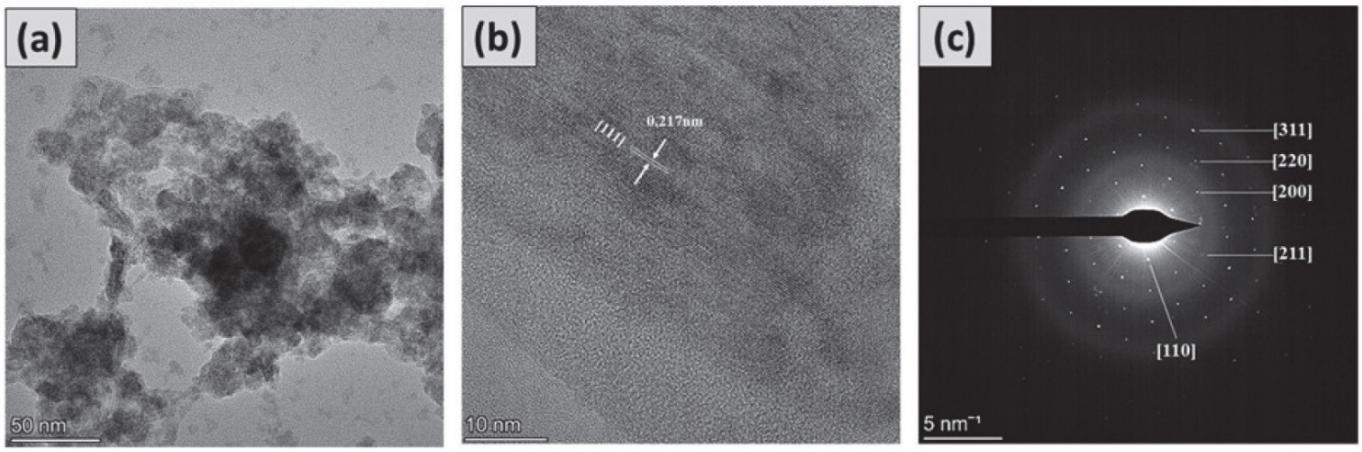


Figure 6. (**a**) TEM, (**b**) HRTEM, (**c**) SAED pattern of DS powder [26].

The fabricated 4 mg of DS-MCPE showed better current sensitivity to detect the AA in a PBS with a pH of 6.8 when compared to 2, 6, 8, and 10 mg of DS-MCPEs. It was determined that the DS-MCPE's active surface area was nearly twice as large as the BCPE's surface area. Additionally, they reported the limit of quantification (LOQ) and limit of detection (LOD), which were determined to be 0.688×10^{-8} M and 0.206×10^{-8} M, respectively. Additionally, they have reported the repeatability, reproducibility, and stability of the DS-MCPE and reported on the effects of scan rate, analyte concentration, pH fluctuations, and interference ions. The graph of various DS-MCPE concentrations, along with their corresponding Ipa and CV, is displayed in Figure 7a,b for 1 mM of AA at BCPE and 4 mg of DS-MCPE [26].

It is confirmed that, in Figure 7a, the Ipa of the 4 mg of DS-MCPE is around twice that of the BCPE. This demonstrates the significance of the modifier, which has a high current sensitivity and can identify the analytes even at low concentrations. The enhanced surface area of the electrode after the modification is the main reason for the higher current. The Ipa of BCPE and DS-MCPE differ from one another, as seen in Figure 7b. When electro-oxidizing 1 mM of AA, BCPE demonstrated an Ipa of 22.5 µA, while 4 mg of DS-MCPE recorded an Ipa of 37.2 µA. The increased surface area and reaction sites in the case of 4 mg of DS-MCPE are responsible for the increased Ipa. Similarly, Rayappa et al. [26] also reported the CV of AA electrochemically oxidized at different pH and scan rates, and different analyte concentrations, as depicted in Figure 8a, Figure 8b, and Figure 8c,

respectively. The pH studies validate the involvement of protons in the electrode response, which shows that increasing the pH from 6 to 6.8 causes Epa to move towards lower values. Participation of protons in the electrode reaction is confirmed by the pH studies, which show the shifting of Epa towards lower values with the increase in the pH from 6 to 6.8. Using the equation below, they have also determined that there are two protons and electrons involved in the electrochemical oxidation of AA:

$$\frac{\Delta E_p}{\Delta pH} = \frac{2.303mRT}{nF} \quad (1)$$

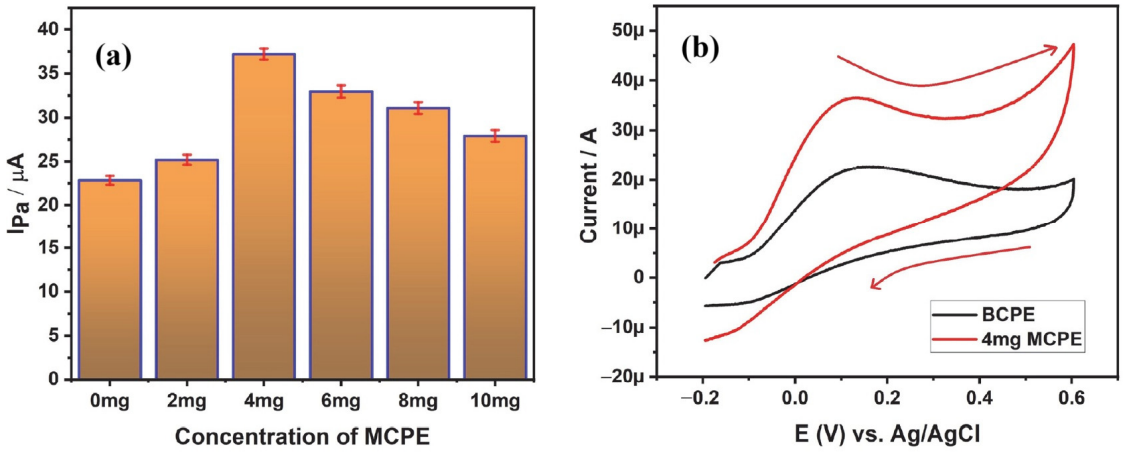


Figure 7. (**a**) DS-MCPE concentration graph with corresponding IPa, (**b**) AA CV at BCPE, and 4 mg of DS-MCPE [26].

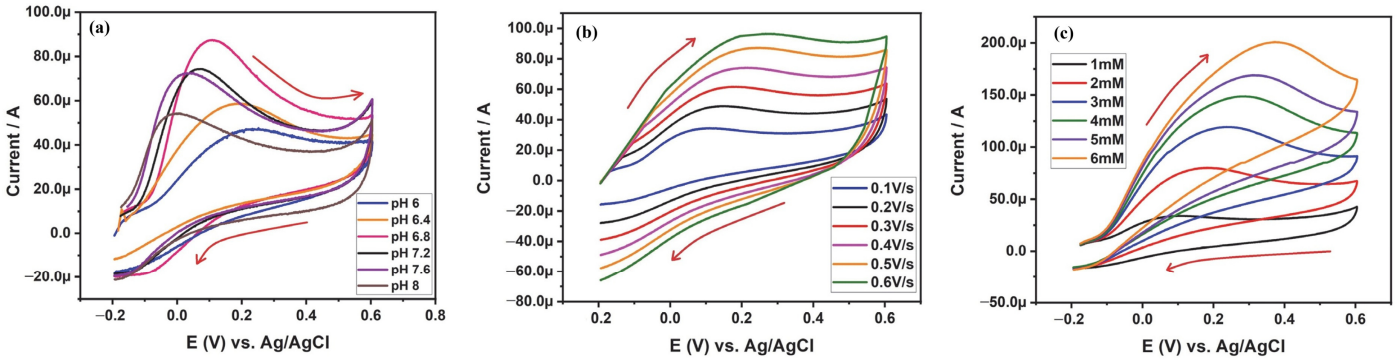


Figure 8. CV of electrochemically oxidized AA at different (**a**) pH PBS, (**b**) scan rates, (**c**) concentrations of AA [26].

Figure 8b demonstrates that raising the scan rate from 0.1 to 0.6 V/s during the electro-oxidation of AA increases the Ipa but decreases the Epa. It is well known that a higher scan rate results in a shorter period to maintain the same charge value, which raises the current. As a result, when AA is electro-oxidized, the anodic peak current value grows as the scan rate does [78]. Fast and direct electron transport between the analyte and the electrode surface is the outcome of this linear increase in Ipa. Similarly, Figure 8c reveals that an increase in the concentrations of the AA from 1 to 6 mM increases the Ipa linearly. Using the standard deviation of the blank CV and the slope obtained after plotting the Ipa vs. concentration of AA, Rayappa et al. [26] calculated LOD and LOQ and the values are 0.206×10^{-8} M and 0.688×10^{-8} M, respectively. Figure 9 shows the electro-oxidation of AA at a pH of 6.8 using DS-MCPE. They have also reported the effect of interfering ions during the determination of AA. They obtained variation of less than

4% in the electrochemical signal of Ipa and this implies that even when different interfering metal ions are present, the DS-MCPE remains extremely stable and selective.

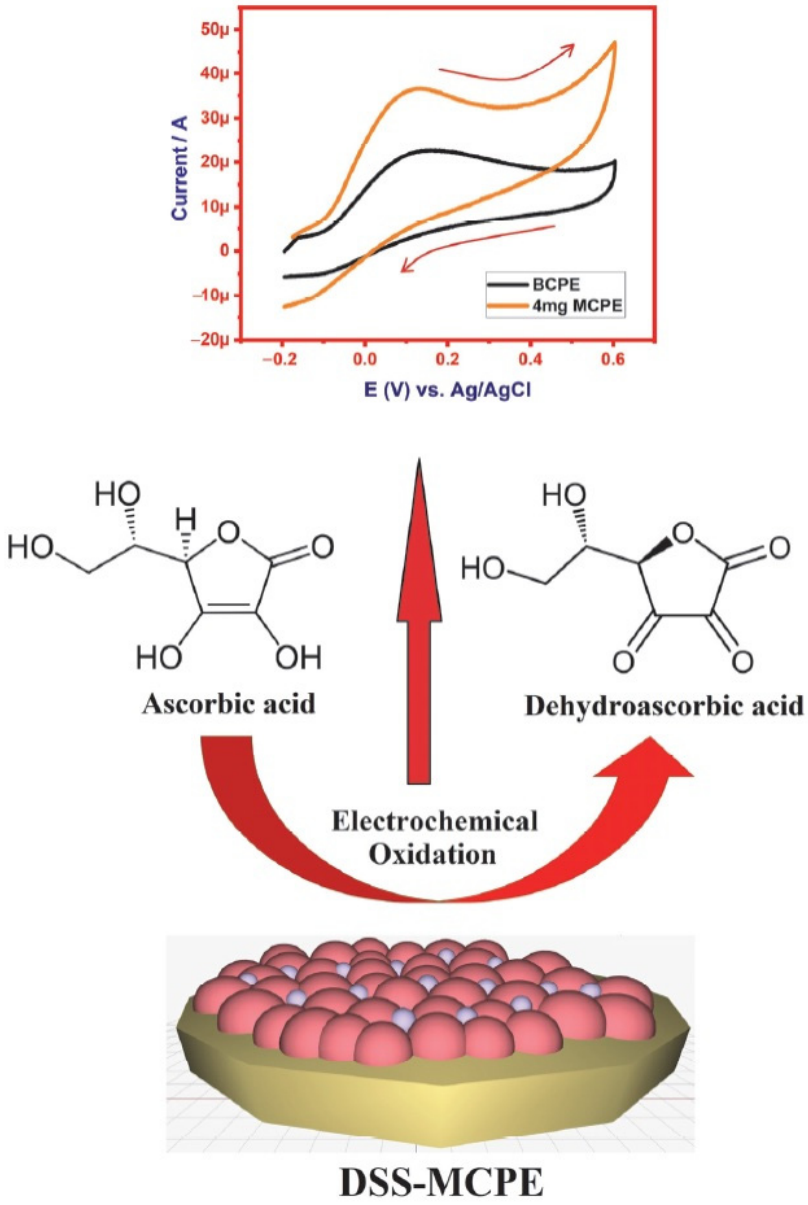


Figure 9. Possible scheme of electrochemical oxidation of AA under DS-MCPE [26].

The repeatability and reproducibility tests were performed five times each by switching the electrode and electrolyte after each run, respectively. The calculated relative standard deviations for reproducibility and repeatability were 3.02% and 2.15%, respectively. These findings suggest that the DS-MCPE is a more reliable and repeatable method for AA molecule detection. Additionally, they investigated the stability of the DS-MCPE by detecting AA in a pH of 6.8 PBS for 50 cycles. The first and final Ipa during the electro-oxidation of AA is recorded to determine the degree of stability. The calculated stability value of 96.98% was obtained and this demonstrates the outstanding stability of the DS-MCPE during the determination of AA.

5.4. Electrochemical Determination of MB (MB)

MB is a synthetic dye, that finds extensive use in both laboratory and medical settings. This dye has a characteristic blue color and is categorized as a thiazine dye

chemically [79,80]. For almost a century, MB has been used for several purposes, including microscopy staining and medicinal uses [81,82]. Apart from its benefits, it has several drawbacks, particularly when used incorrectly or in conjunction with specific medical problems. The biggest worries are the possibility of toxicity at high dosages, serotonin syndrome when taken with certain drugs, and hemolysis in people with G6PD deficiency. Like any drug or substance, MB should be used with caution and under the supervision of medical specialists [83–85]. The chemical structure of MB is shown in Figure 10.

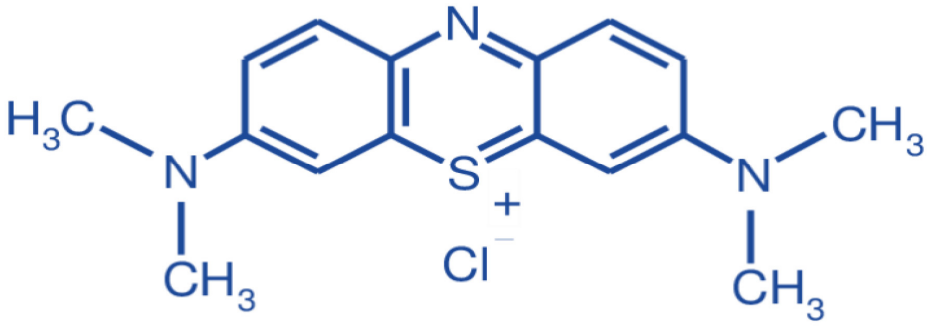


Figure 10. Chemical structure of MB [86].

MB is used as a coloring agent in a variety of sectors, such as textiles, leather, and paper. However, the significant MB dye discharge by these industries as wastewater into the surface and groundwater causes environmental issues, resulting in adverse effects on ecosystems and health issues [83–86]. The electrochemical oxidation of MB by cyclic voltammetry method is considered one of the best suitable methods. Because of its ease of use, sensitivity, low cost, and speed, this method provides detailed information about the electrochemical determination of MB dye, making it very useful in the biomedical sector [87–91].

Therefore, Rayappa et al. [27] determined the MB dye by cyclic voltammetry method using DS-MCPE. Figure 11a,b represents the Ipa of MB obtained at various concentrations of DS-MCPE and the CV of BCPE and DS-MCPE, respectively. From the figure, it is confirmed that 2 mg of DS-MCPE has shown excellent current response compared to BCPE and MCPE has shown more than 7 times the Ipa of BCPE. This confirms the importance of a modifier like DS powders [27].

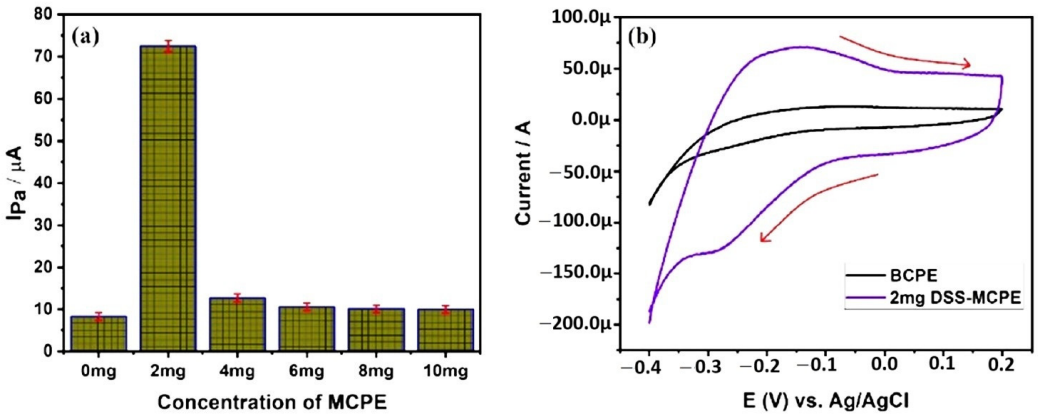


Figure 11. (**a**) Graph of Ipa at various concentrations of DS-MCPE, (**b**) CV of BCPE, and 2 mg of DS-MCPE [27].

On the other hand, the authors also reported the effect of pH variation, the effect of scan rate, and the effect of MB concentrations, and their respective CVs are depicted in Figure 12a–c. An increase in the scan rate and increase in the concentrations of MB increases

the Ipa, as we discussed earlier. When the pH rises from 6 to 8, the Epa shifts to lower values. This indicates that the electrochemical oxidation of MB involves protons.

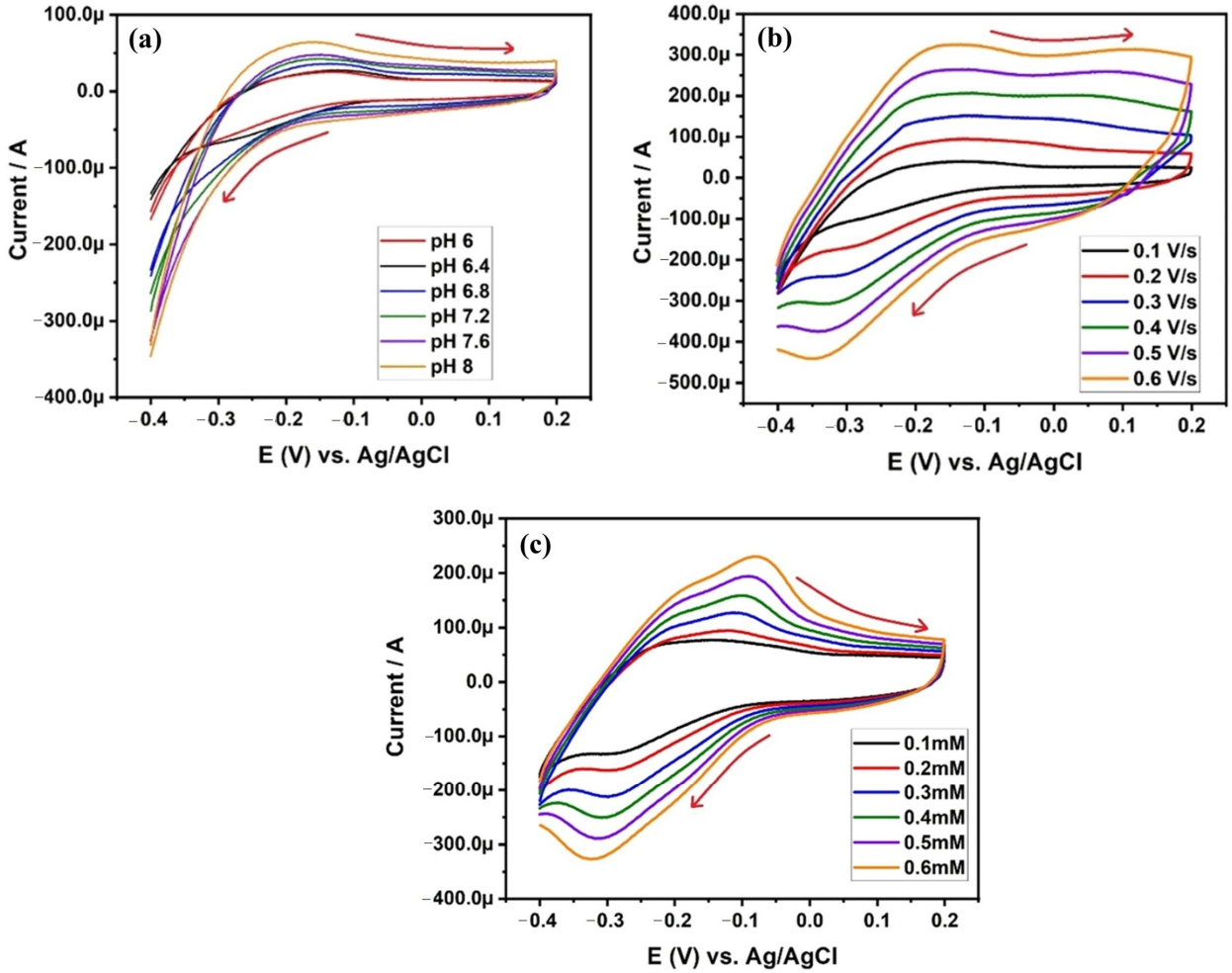


Figure 12. CV of electrochemically oxidized MB at different (**a**) PBS pH, (**b**) scan rates, (**c**) concentrations of MB, respectively, at DS-MCPE [27].

The calculated values of LOD and LOQ are 0.222×10^{-8} and 0.74×10^{-8} M, respectively [27]. Figure 13 shows the potential mechanism of the electrochemical reaction of MB using DS-MCPE. Several metal ions (Na^+, Cu^{2+}, Fe^{2+}, Mg^{2+}, Fe^{3+}, K^+) and bioactive compounds were used as the interferents and investigated up to what extent these interferents can affect the Ipa of MB. Notably, the Ipa and Epa of MB did not significantly change either positively or negatively, confirming DS-MCPE's strong selectivity. Furthermore, DS-MCPE showed exceptional stability even after 50 cycles of continuous 0.1 mM MB detection at pH 8, demonstrating its long-lasting effectiveness under electrochemical testing. Given the improved stability and sensitivity of the DS-MCPE electrode, it is a potential candidate for determining MB dye and can be incorporated into portable platforms for quick analysis. Future research will concentrate on improving device mobility and fabrication procedures and addressing pragmatic issues.

5.5. Electrochemical Determination of Rhodamine B (Rh B)

Rhodamine B is a synthetic dye that belongs to the Rhodamine family. It is frequently used in textile dyeing, biological research, and other industrial operations as a fluorescent tracer [92–94]. It has a fused tricyclic structure with nitrogen atoms and a benzene ring joined to a carboxyl group, as shown in Figure 14. When solid, it is a dark red or purple

powder; when dissolved in water, it will show a pink color. Because of its fluorescent qualities, it can be used in a variety of processes, including DNA measurement, flow cytometry, and microscopy [95–97].

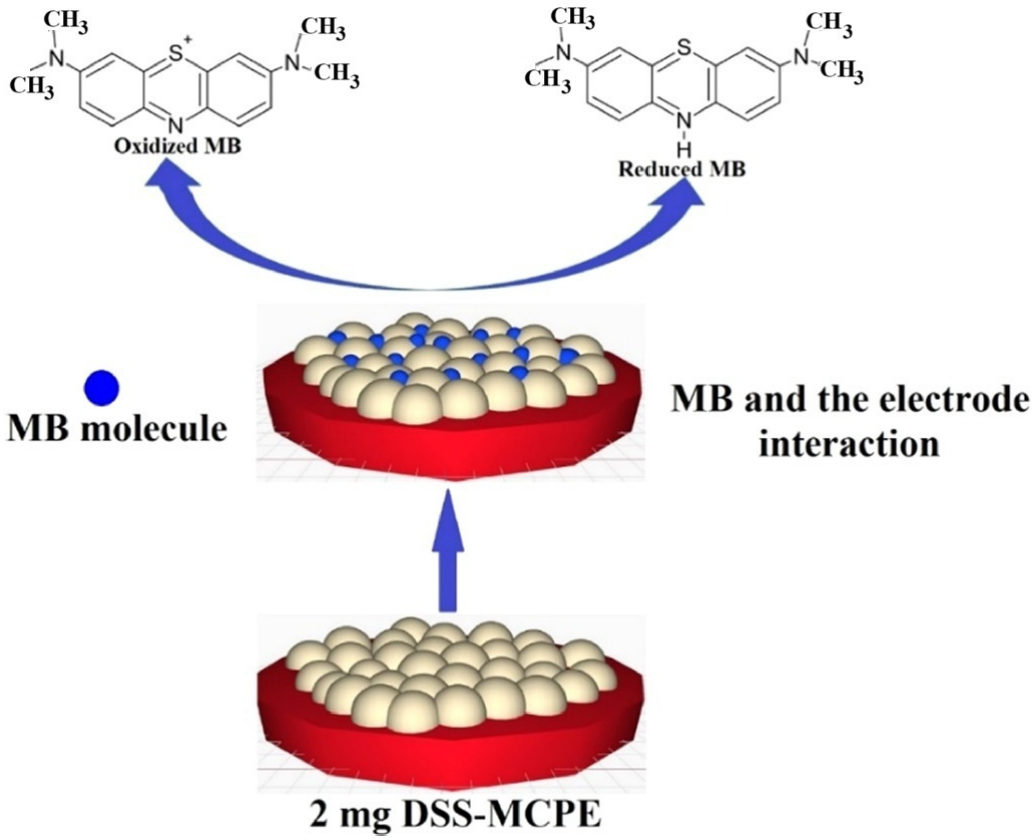


Figure 13. Possible scheme of electrochemical oxidation of MB at DS-MCPE [27].

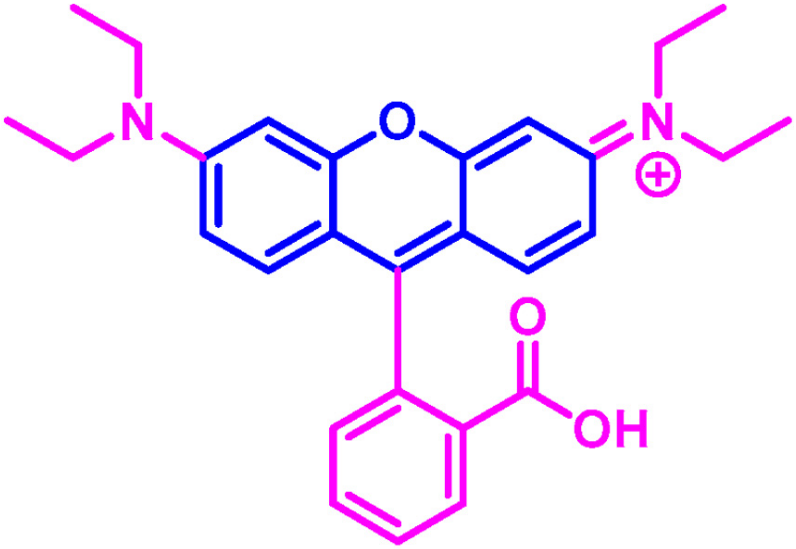


Figure 14. Chemical structure of Rhodamine B [98].

Rhodamine B is utilized extensively in science and industry, but its possible harmful effects on the environment and human health should not be disregarded. Long-term use of Rhodamine B can cause chronic diseases like kidney and liver damage, a person can develop vomiting and abdominal pain, and excessive use can affect the human reproduction system [92–96]. It is highly carcinogenic in nature and increases the risk of cancer. To reduce

the possible danger, proper handling, safety precautions, and compliance with rules are crucial. Further study is required to completely comprehend the long-term effects on human health and the environment to appropriately assess and lessen the risks connected with its widespread use. Keeping in mind the adverse effects of Rhodamine B, we must develop a system that can determine Rhodamine B even at small concentrations.

Shashanka et al. [28] attempted to study their electrochemical properties using DS-MCPE using cyclic voltammetry technique and reported excellent results. Figure 15a,b represents the graph of Ipa reported at different concentrated DS-MCPEs and the CV of BCPE and DS-MCPE, respectively. According to the figure, 6 mg of DS-MCPE has shown more than 2 times the Ipa of BCPE because of increased surface area and reaction sites after modification. The authors have also calculated the active surface areas of 6 mg of DS-MCPE and BCPE and the values were found to be 0.302 and 0.761 cm^2, respectively. This shows the importance of the modification of the CPEs.

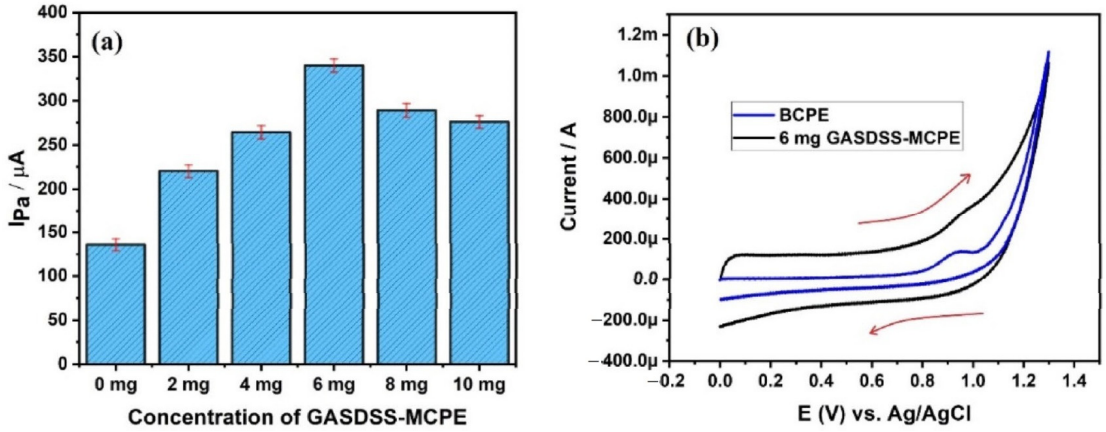


Figure 15. (**a**) Plot of Ipa at various concentrations of DS-MCPE, (**b**) CV of BCPE, and 6 mg of DS-MCPE [28].

On the other hand, the authors have also studied the consequence of scan rate and the analyte's concentrations on the electrochemical oxidation of Rhodamine B and represented as a CV in Figure 16a and Figure 16b, respectively. During the electrochemical oxidation of Rhodium B, an increase in scan rate and analyte concentration increases the current response. This is because it takes less time to maintain the charge values at faster scan rates and because the DS-MCPE surface and the analyte interact strongly, increasing electron mobility. For the 6 mg of DS-MCPE, the determined LOD and LOQ were 0.378 µM and 1.260 µM, respectively.

They have also reported that interference like vanillin, FA, uric acid, methylene blue, methyl orange, K^+, Fe^{2+}, and Mg^{2+} does not affect the current response of the 6 mg of DS-MCPE during the electrochemical oxidation of Rhodamine B. They have excellent stability, repeatability, and reproducibility results for the DS-MCPE, and, therefore, DS-MCPE is one the very important and potential electrodes that can be used to determine Rhodamine B in real samples. The electrochemical oxidation of Rhodamine B is shown in Figure 17.

5.6. Electrochemical Determination of Folic Acid (FA)

FA is essential for many body processes, particularly the creation and growth of cells. It is made artificially and can be found in supplements, fortified foods, and some natural foods such as fruits, vegetables, whole grains, and legumes [99,100]. The synthetic form of folate found naturally in food is called FA. During pregnancy, infancy, and adolescence, FA is crucial because the body needs it to manufacture DNA, make red blood cells, and maintain healthy cell division [101–104]. FA is a pteroylglutamic acid derivative, which

consists of a pteridine ring, para-aminobenzoic acid, and glutamic acid, and its chemical structure is shown in Figure 18.

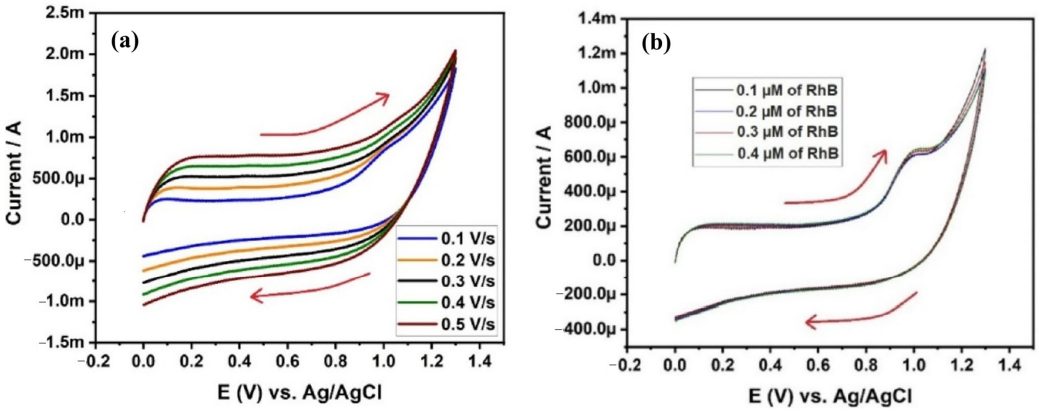


Figure 16. CV of Rhodamine B using 6 mg of DS-MCPE at different (**a**) scan rates and (**b**) concentrations of Rhodamine B analyte [28].

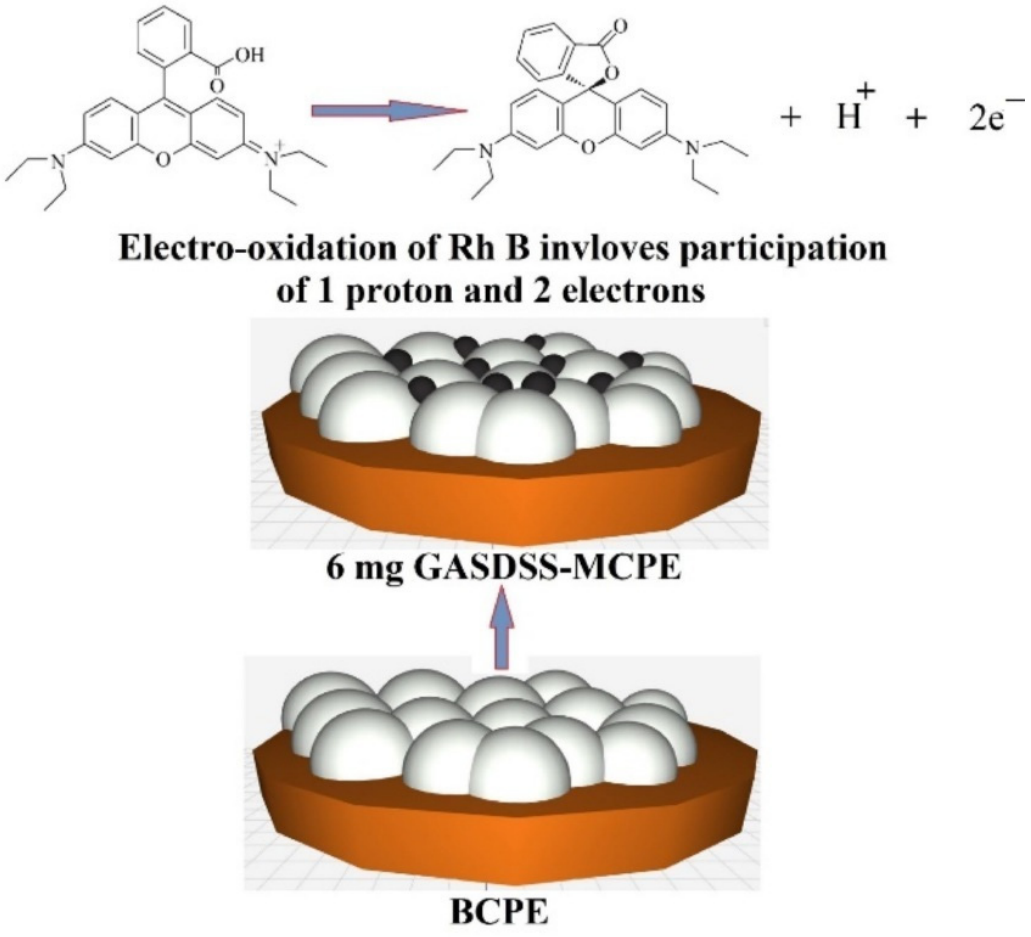


Figure 17. Possible scheme of electrochemical oxidation of Rhodamine B at DS-MCPE [28].

FA is very necessary to maintain cognitive function and mental health, and it reduces depression. Some studies also revealed that FA consumption can reduce the risk of colorectal and cervical cancer by promoting DNA stability and repair. Deficiency of FA during pregnancy can lead to spina bifida and anencephaly (improper growth of the spine and brain, respectively). Diseases like cardiovascular defects, immune system malfunction, dementia, depression, and macrocytic and megaloblastic anemia are caused because of FA

deficiency. A crucial nutrient, FA has a wide range of effects on human health, especially in preventing birth abnormalities, promoting cellular function, and preserving general well-being. Its extensive use as a supplement and in food fortification highlights how crucial it is to contemporary healthcare and illness prevention [99–104]. Like any nutrient, though, balance is essential because both an excess and a shortage can cause health issues. Therefore, we need to determine the FA frequently, there are many analytical and electrochemical methods available to determine it, but cyclic voltammetry has proved to be one of the best techniques to determine FA.

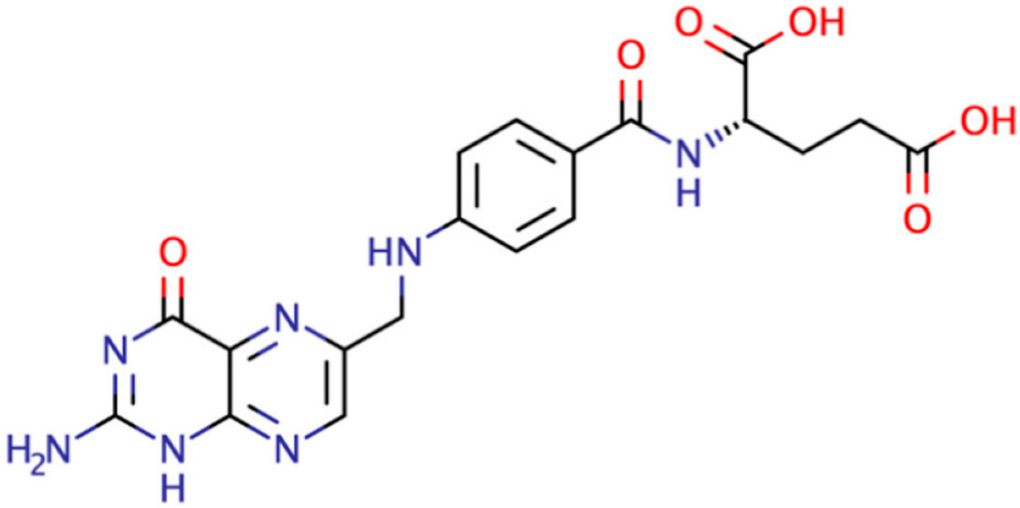


Figure 18. Chemical structure of FA [105].

Shashanka et al. [29] reported the determination of FA using DS-MCPE by cyclic voltammetry method. As we know, optimization of the experimental condition is very important to obtain good results. Authors fabricated DS-MCPE at different concentrations of DS powders as a modifier. Among, 2, 4, 6, and 8 mg of DS-MCPE, 4 mg of DS-MCPE has shown excellent current response during electrochemical oxidation of FA compared with the BCPE, as shown in the CV of Figure 19a. This is because of the increase in the surface area and the reactive sites due to the enhanced surface roughness after modifying the BCPE with 4 mg of DS powders. They have also studied the effect of scan rate and the effect of concentration variation of FA, and their respective CVs are shown in Figure 19b,c.

An increase in the scan rate and the concentration variation of FA increases the Ipa, respectively, due to the reduced time to keep the charge values at higher scan rates and the increased number of FA molecules at higher concentrations. This will create a strong electrochemical reaction between the DS-MCPE and the analyte FA, as a result of which the movement of electrons will increase, and thus increase the Ipa. On the other hand, an increase in pH from 5.7 to 8 will make Epa of FA shift towards negative potential. This confirms the participation of protons in the electrochemical oxidation of FA. It is possible to determine the number of electrons and protons participating in the electrochemical reaction of FA by investigating the effect of pH variation. As per the values mentioned in the article [29], we calculated the number of protons and electrons involved, and the values were found to be almost 2. At last, they have concluded that the fabricated FA sensor could be a potential sensor to diagnose FA deficiency diseases and they have reported all the electrode reactions are adsorption controlled.

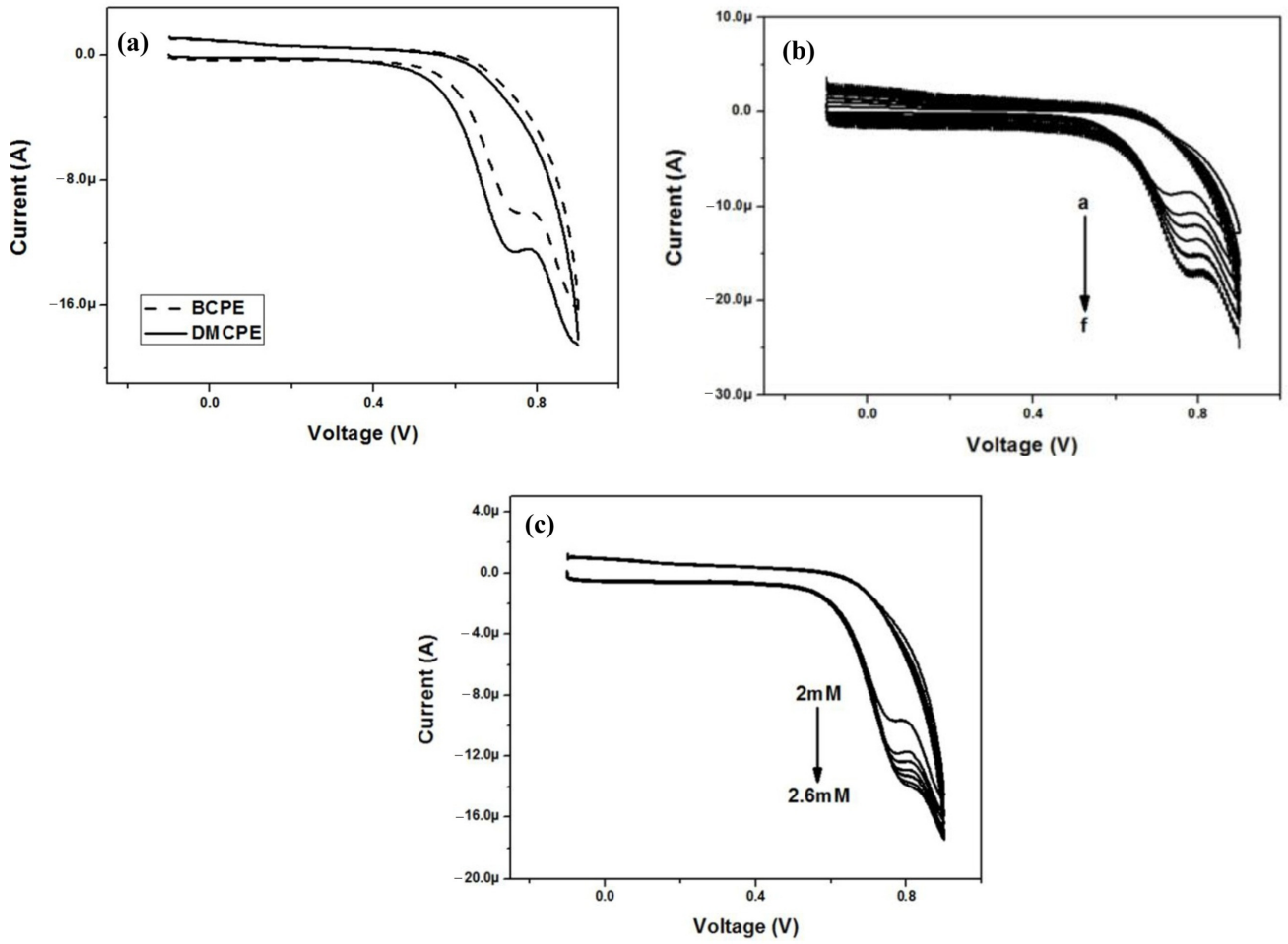


Figure 19. CVs obtained during the electrochemical oxidation of FA using (**a**) DS-MCPE and BCPE, (**b**) at different scan rates (a = 50, b = 100, . . ., f = 300 mV/s), (**c**) at different concentrations of FA [29].

6. High-Entropy-Alloy-Modified Carbon Paste Electrode (HEA-MCPE)

6.1. Introduction to High-Entropy Alloys (HEAs)

High-entropy alloys (HEAs) are the novel grades of modern alloys, which have attracted a lot of interest lately because of their special qualities and potential for a variety of uses. HEAs are made up of five or more major elements, each in large proportions (generally 5–35% by atomic percentage), in contrast to ordinary alloys, which are often made up of a single dominant element and a few alloying elements [106,107]. This produces a multi-phase, multi-configuration, extremely complex microstructure that combines good mechanical, thermal, chemical, and electrochemical properties [108–111].

The phrase "high entropy" describes the system's high configurational entropy, which is the outcome of mixing several different components. This opens the door to the creation of new solid-solution phases, including HCP, BCC, and FCC structures [112]. Despite the existence of many major elements, one of the main features of HEAs is their ability to create single-phase solid solutions. In contrast, secondary phases are frequently formed by extra components in typical alloys. Strength and hardness are boosted by the huge number of elements in HEAs, which stabilizes the solid solution phase at room temperature [113,114]. One of the popular, effective modern methods to prepare HEAs is mechanical alloying [110]. A graphical representation of preparing HEAs by the ball-milling method is depicted in Figure 20.

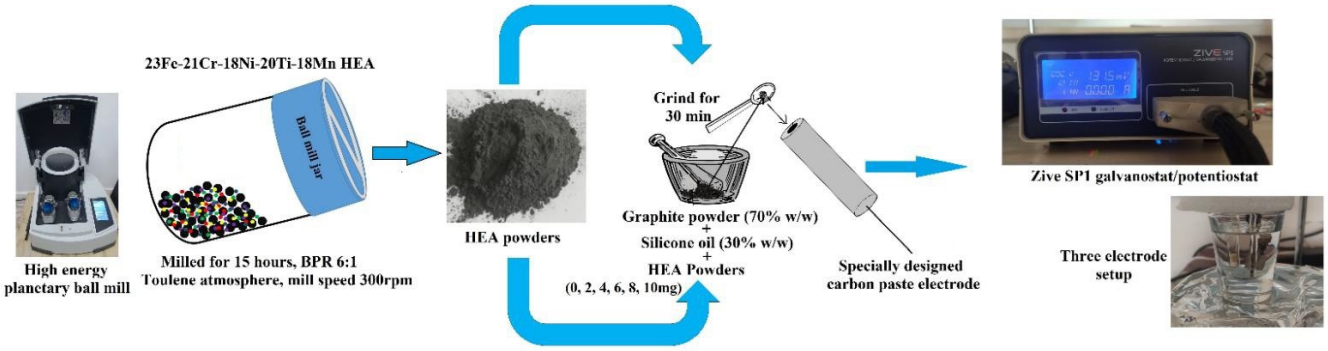


Figure 20. Graphical representation of ball milling of HEA and the fabrication of HEA-MCPE [30].

Figure 21a,b depicts the XRD and SEM images of ball-milled HEAs for 15 h from 0 h [30]. It has several advantages over traditional metallurgical methods. HEAs exhibit high mechanical strength, toughness, ductility, high resistance to corrosion, heat, and wear, and excellent magnetic, electrical, and electrochemical properties. Therefore, they are mainly used in aerospace, energy, coating, biomedical, defense, and automatic sectors. However, HEAs still have enormous potential to overcome many of the drawbacks of conventional alloys, like defining the phase diagrams, low cost, product designing, etc., and open the door to new technological advancements, as long as research and development continue. One of the recent novel applications of HEA is as an "electrocatalyst" to determine various dyes and bioactive compounds by cyclic voltammetry. Very few articles have been published about the electrocatalytic properties of HEAs to investigate redox reactions of various compounds, and we have reviewed a few of them and discussed how HEA plays an important role in acting as AA, methyl orange, and MB sensors.

6.2. Electrochemical Determination of AA

We discussed the importance, properties, applications, and effects of AA on human health earlier in this review article. We will discuss how HEA will help to determine the AA. Shashanka et al. [30] reported the excellent electrochemical properties of HEA powders and their potential use as an AA sensor. They have studied the effect of HEA as a modifier in the CPEs by varying the concentrations of the HEA during the electrochemical oxidation of AA. Among 2, 4, 6, 8, and 10 mg of modified HEA-MCPE, 8 mg of HEA-MCPE has shown an excellent current response, as shown in Figure 22a, and the CV of BCPE and HEA-MCPE in Figure 22b, respectively.

Using the Nernst equation, they determined the active surface area of HEA-MCPE and BCPE, which came out to be 0.0027 cm^2 and 0.0014 cm^2, respectively; this means that after the modification of CPE, its active surface area increased almost 2 times. This will increase the reactive sites and increase the mobility of electrons between the electrode and the AA. Therefore, always MCPEs will show a higher current response than BCPEs in most of the analytes. CVs obtained for the variation in pH and concentration of the AA are shown in Figure 23a and Figure 23b, respectively [30].

As per the figure, as the PBS pH increases from 6 to 8, the Epa is decreasing. On the other hand, concentration variation studies reveal that an increase in the concentrations of AA increases the Ipa linearly. At last, they have concluded that the manufactured HEA-MCPE has demonstrated excellent sensitivity and selectivity in identifying AA. In the medical field, the current electrode may be used as a sensor to diagnose disorders caused by AA deficiency. They have reported that the diffusion phenomenon controls the electrode processes that occur during the electrochemical oxidation of AA.

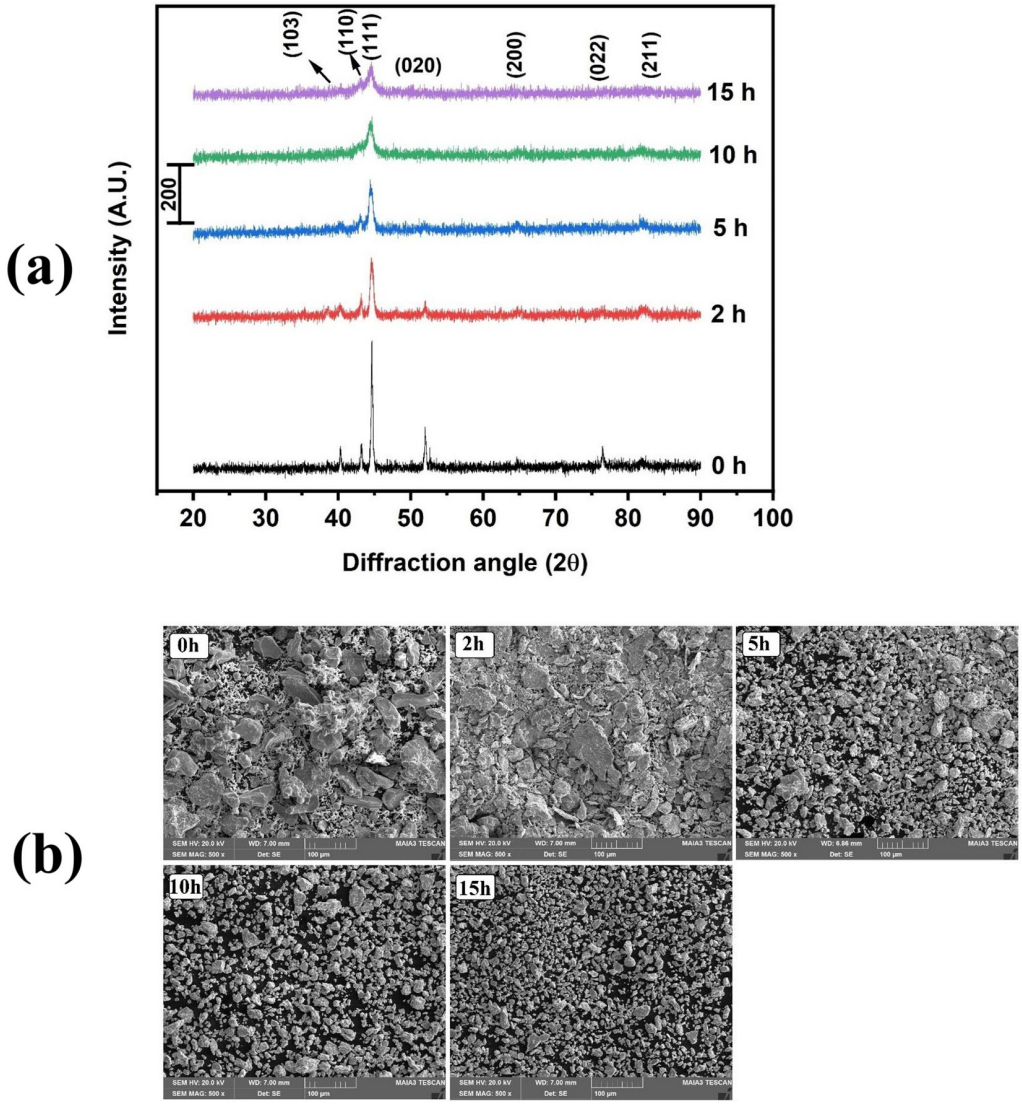


Figure 21. (**a**) XRD and (**b**) SEM of 0 to 15 h ball-milled HEA powders with regular time intervals [30].

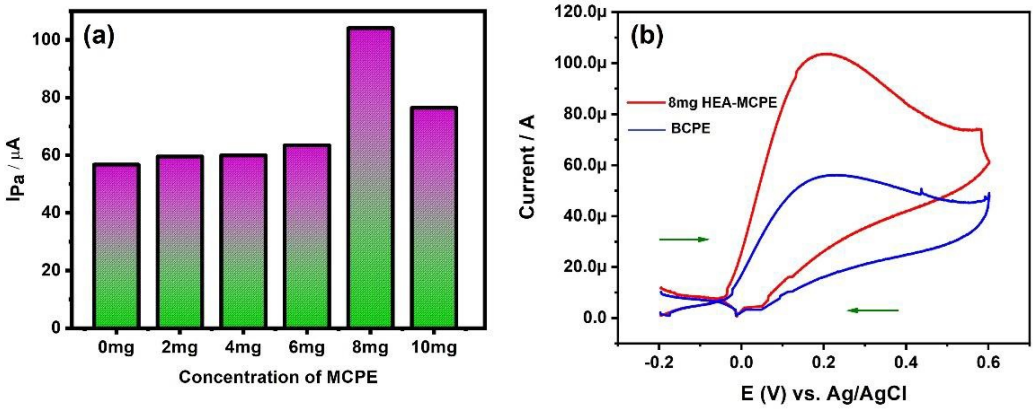


Figure 22. (**a**) Ipa at various concentrations of HEA-MCPE, (**b**) CV of BCPE, and 8 mg HEA-MCPE [30].

6.3. Electrochemical Determination of Methyl Orange

Shashanka et al. [31] have reported the use of HEA powders as a modifier in CPEs to determine methyl orange using CV. Figure 24 is the pictorial representation of the experiment carried out in the article [31].

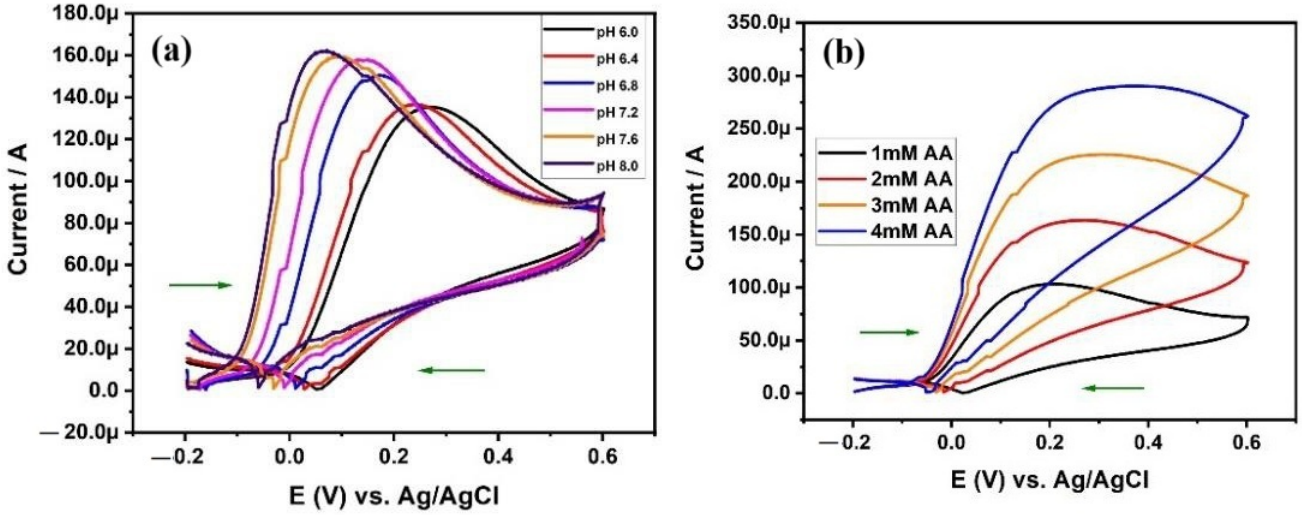


Figure 23. CVs electrochemical oxidation of AA using HEA-MCPE at different (**a**) pH of PBS and (**b**) concentrations of AA analyte [30].

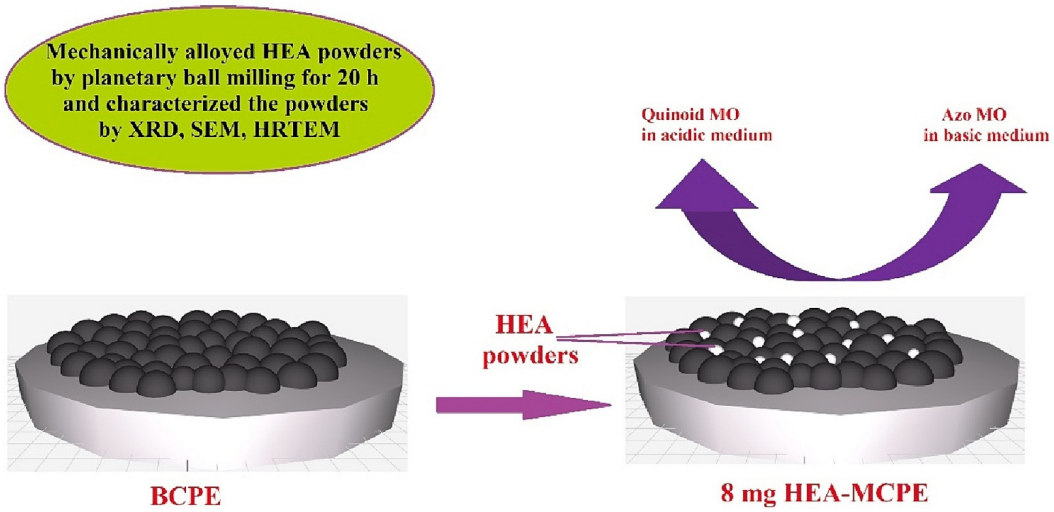


Figure 24. Pictorial representation of fabrication of HEA-MCPE and the electrochemical oxidation of methyl orange [31].

As seen in Figure 25a, they synthesized 2, 4, 6, 8, and 10 mg of HEA-MCPE and noted the corresponding Ipa achieved for the electrochemical oxidation of methyl orange. The graph indicates an increase in surface area and reactive sites up to 8 mg HEA-MCPE, followed by a decrease at 10 mg HEAMCPE. It also shows a rise in Ipa till 8 mg HEA-MCPE, after which it abruptly declines. Figure 25b depicts the over plot of CVs of a blank (without the analyte methyl orange), BCPE, and HEA-MCPE. There is an increase of 4 times the Ipa of 8 mg HEA-MCPE compared to BCPE. The pH studies revealed the participation of protons in the electrochemical oxidation of methyl orange and the calculated number of protons is 2.

The CV obtained for different pH solutions is shown in Figure 26a and its linear regression equation obtained is as follows: Ep (V) = 1.1452 − (0.060) pH (V/pH) (R^2 = 0.9980). The reported slope obtained after plotting a graph of Epa vs. pH is 0.0603 and the value is very close to the Nernst relation value of 0.059 V/pH. This confirms the participation of an equal number of electrons and protons during the electrochemical reaction. They have also performed the variation of the scan rate and the methyl orange and reported their effect on the Ipa of methyl orange, and their respective CVs are shown in Figure 26b,c. Using the Ipa values of Figure 26c, the authors have calculated the LOD and LOQ, and the values were

found to be 1.14 nM and 3.8 nM, respectively. The investigations related to the effect of interferents, stability, reproducibility, and repeatability have shown excellent temperament of the HEA-MCPE. This HEA-MCPE can be a potential candidate in the future to detect methyl orange in wastewater, food products, etc. [31].

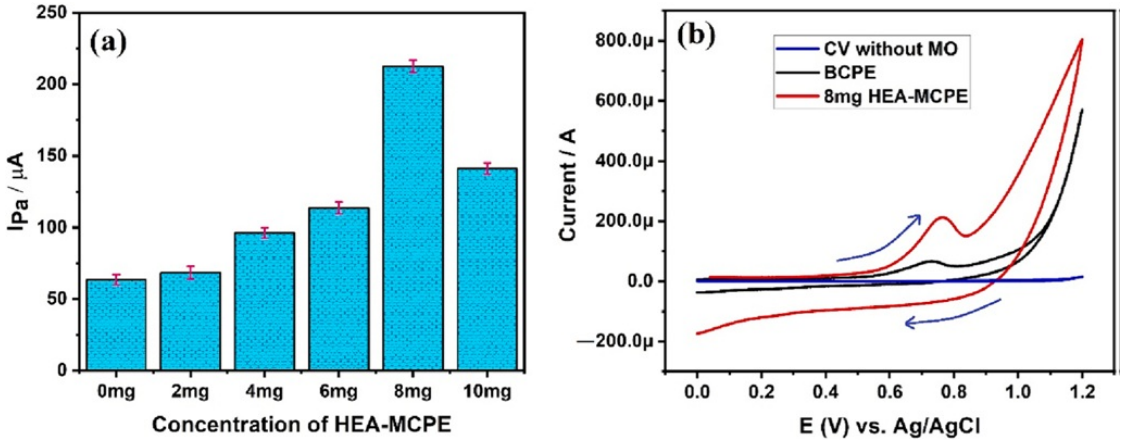


Figure 25. (**a**) Graph of respective Ipa reported at different concentrations of HEA-MCPE, (**b**) CV of a blank (without the analyte methyl orange), BCPE, and HEA-MCPE [31].

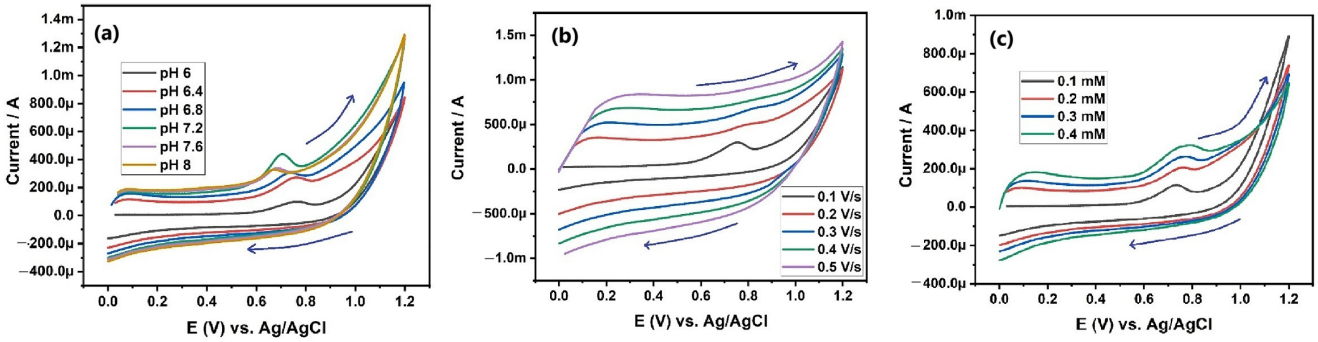


Figure 26. CVs of electrochemical oxidation of methyl orange using HEA-MCPE at different (**a**) PBS of pH, (**b**) scan rates, (**c**) concentrations of methyl orange analyte [31].

6.4. Electrochemical Determination of Methylene Blue

The accuracy, selectivity, sensitivity, repeatability, and reproducibility are further increased by modifying the CPE with ball-milled HEA powders. Shashanka et al. [32] prepared different concentrated HEA-MCPE (2, 4, 6, 8, and 10 mg) and recorded the respective Ipa during the electrochemical redox reaction of the MB and its graphical experimentation is as given in Figure 27 and the Ipa plotted the graph concerning different modifier concentration is as shown in Figure 28a. Among all, 4 mg HEA-MCPE has shown a maximum current response than others. Figure 28b indicates the CVs of BCPE and the 4 mg HEA-MCPE, and from the figure, it is confirmed that the Ipa of HEA-MCPE is 5 times more than the Ipa of BCPE. Therefore, they have used 4 mg HEA-MCPE for further studies.

Figure 29a depicts the CV of MB oxidized at different PBS of pH 6 to 7.6 at a scan rate of 100 V/s. Authors have plotted the Epa vs. different pH and their plot follows the linear regression equation as follows: Ep (V) = 0.5235 − (0.0651) pH(V/pH) (R^2 = 0.9938). This confirms that the electron mobility during the electrochemical redox reaction of MB mainly depends upon the protons. The slope obtained is 0.0651 and it is almost equal to the theoretical standard value of 0.059 V/pH. On the other hand, Figure 29b shows the CV obtained at different concentrations and the Ipa increases linearly. According to the results obtained during the scan rate variations, the mass transfer process is diffusion-controlled.

They concluded that the prepared HEA-MCPE might be potentially used as an electrode to detect different dyes, medications, hazardous heavy metals, pesticides, etc. This will give metallurgists and mechanical engineers a new field of study to use different alloy powders for a range of electrocatalytic applications.

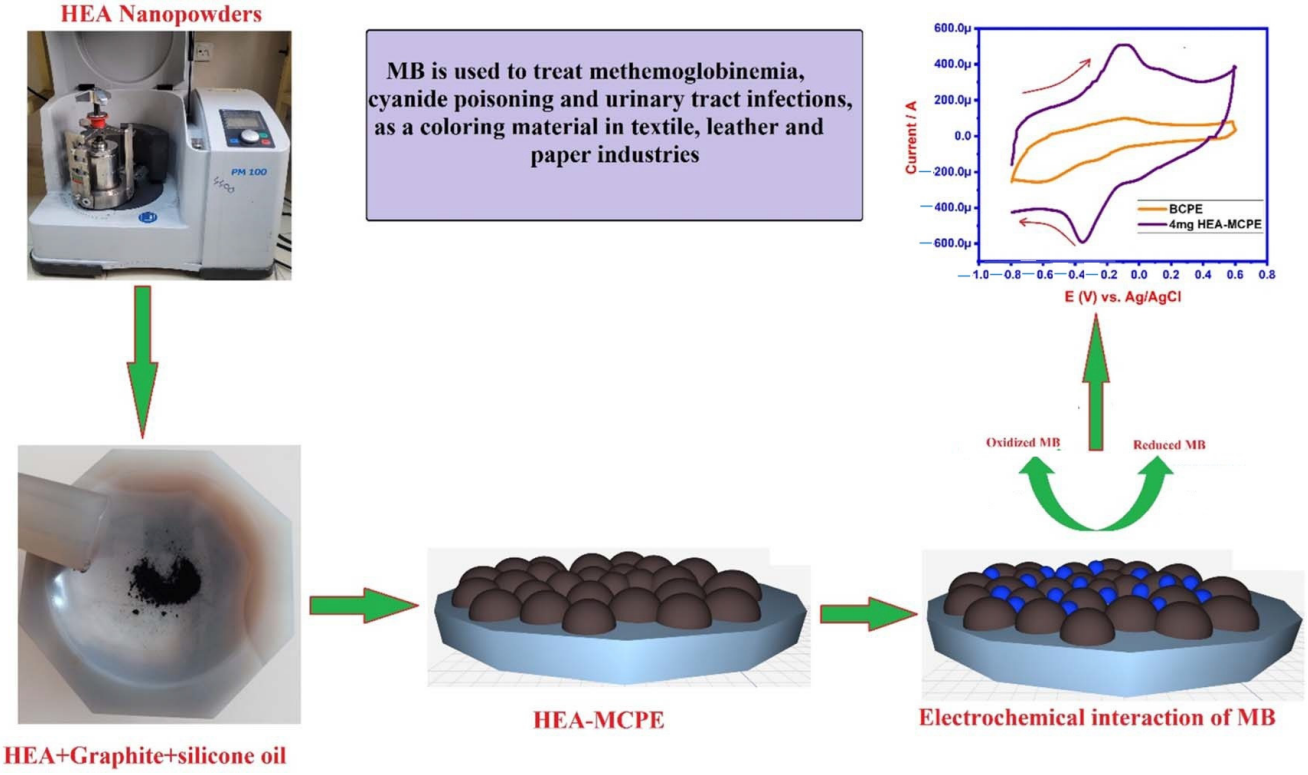


Figure 27. Pictorial representation of fabrication of HEA-MCPE and the electrochemical oxidation of MB [32].

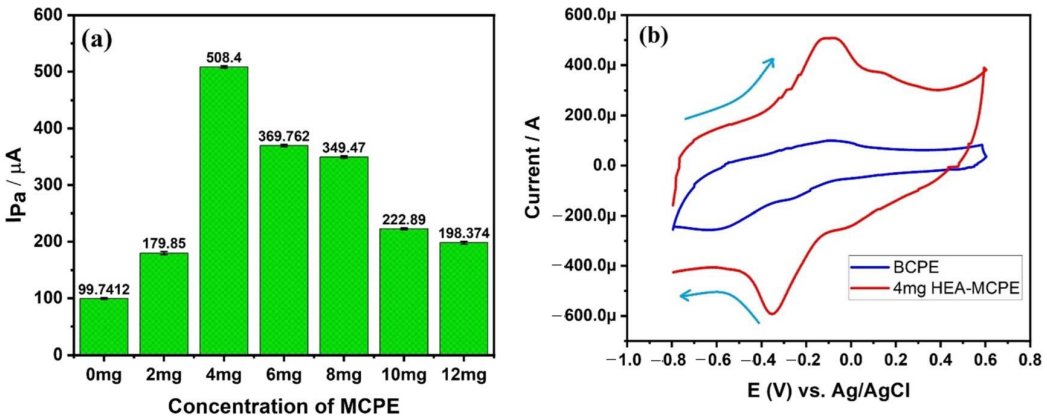


Figure 28. (**a**) Plot of Ipa vs. different concentrations of HEA-MCPE, (**b**) CV of BCPE, and 4 mg HEA-MCPE [32].

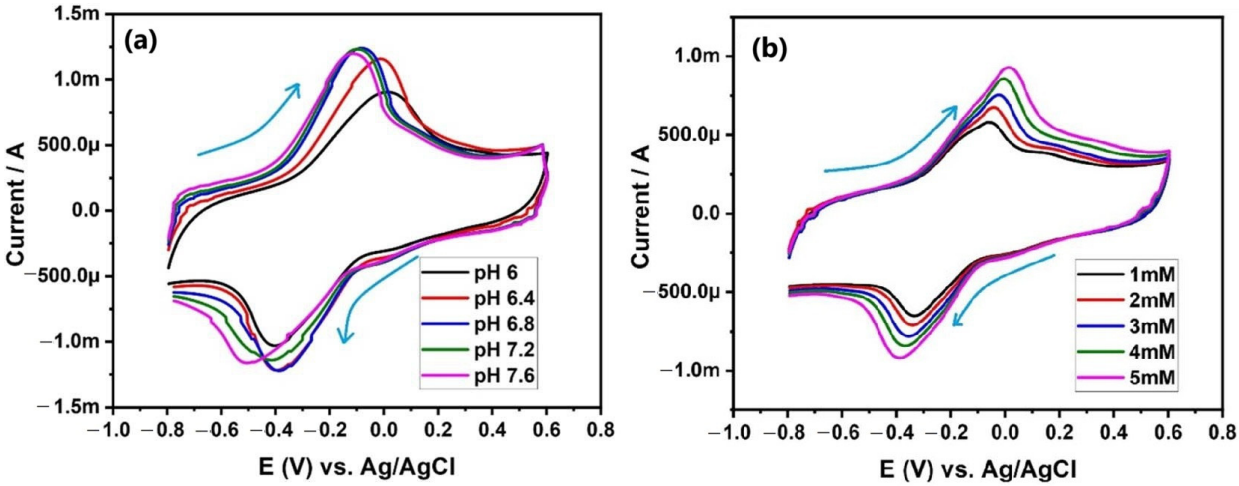


Figure 29. CVs of electrochemical redox reaction of MB under HEA-MCPE at different (**a**) PBS of pH, (**b**) concentrations of MB analyte [32].

7. Shape-Memory-Alloy-Modified Carbon Paste Electrode (SMA-MCPE)

7.1. Introduction to Shape-Memory Alloys (SMAs)

A special class of metallic materials known as shape-memory alloys (SMAs) can revert to a predetermined shape in response to a specific stimulus, like heat. They are categorized as "smart materials" because of their exceptional characteristics [115,116]. When exposed to stress or temperature fluctuations, SMAs go through a phase transformation that allows them to regain their former structure. One of the main characteristics of SMAs is this phenomenon, which is known as the shape-memory effect [117–120]. Although nickel–titanium (NiTi) alloys are widely used SMAs, other alloys, including copper–aluminum–nickel (Cu-Al-Ni) and iron-based SMAs, are also used as SMAs. NiTi alloys are also called nitinol and they undergo the reversible phase transition between a low-temperature and a high-temperature phase. The phase transformation mainly depends upon the temperature and they exhibit superelasticity, high damping capacity, excellent electrochemical properties, biocompatibility, fatigue resistance, etc. [116–120]. Therefore, they are used in stents, surgical instruments, orthodontics, actuators, automotive, aerospace, electronics, defense, microelectromechanical systems (MEMS), and electrochemical sensor applications.

7.2. Preparation of Shape-Memory Alloys (SMAs) by Mechanical Alloying

Shape-memory alloys can have their qualities improved and customized with the help of mechanical alloying. It makes it possible to precisely manipulate the microstructure and composition of the material, which can result in enhanced performance in a variety of demanding applications, superelasticity, and increased shape-memory effects [33]. If we control the basic ball-milling issues like oxidation and phase stability and perform milling optimization before the start of the actual milling, then we can fabricate high-quality nitinols. Mechanically alloyed nitinols possess excellent porosity, high surface area, and surface energy; therefore, nitinols could be potential electrocatalysts. If we disperse the elements like Hf, Cu, carbon nanotubes, and graphenes in small amounts to NiTi composition, then their properties will be improved further.

7.3. Electrochemical Determination of Dopamine

Shashanka et al. [33] investigated the electrocatalytic properties of ball-milled nitinols dispersed with Hf, and the graphical representation of the whole experiment starting from the milling to fabrication of NiTiHf-MCPE is shown in Figure 30. They have investigated the phases present in the alloy at different milling times from 0 to 20 h by XRD and it is

given in Figure 31. As per the XRD, we believe 20 h of milling time is required to obtain highly refined SMA powders. Similarly, the progress of milling at different milling times is further investigated by SEM and EDS analysis as shown in Figure 32. The figure confirms the gradual decrease in the particle size from 0 to 20 h of ball milling with the irregular shape of the powders.

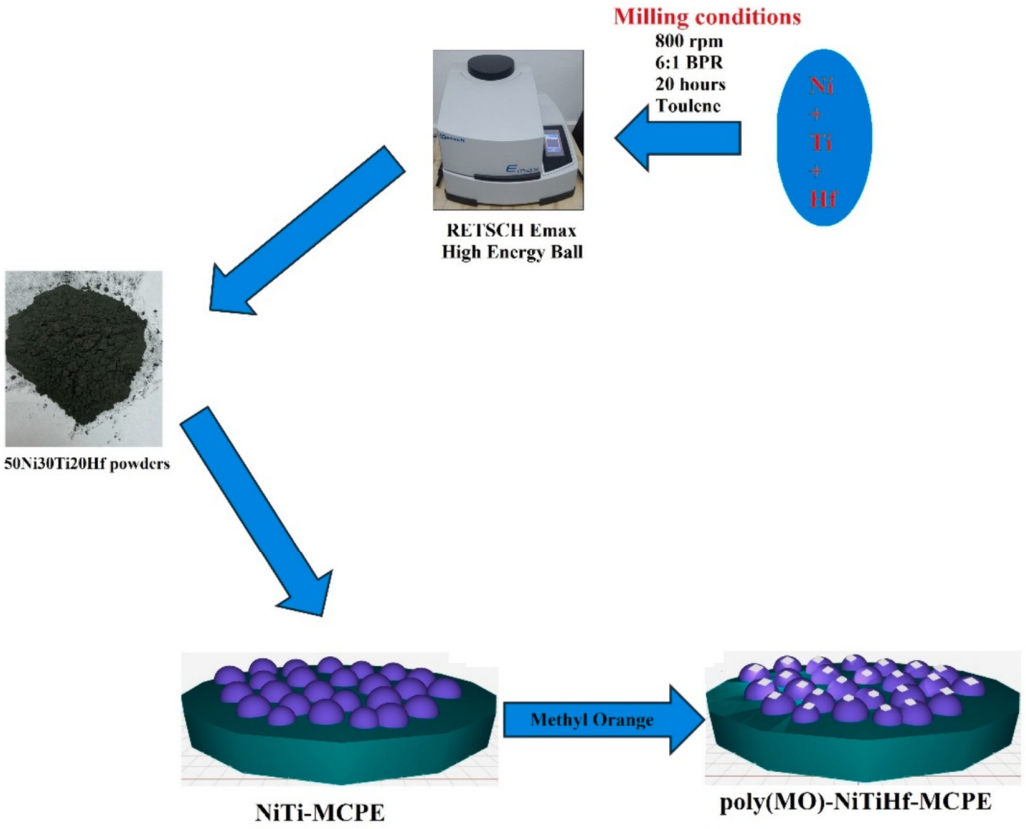


Figure 30. Pictorial representation of whole experiment starting from the milling to fabrication of NiTiHf-MCPE [33].

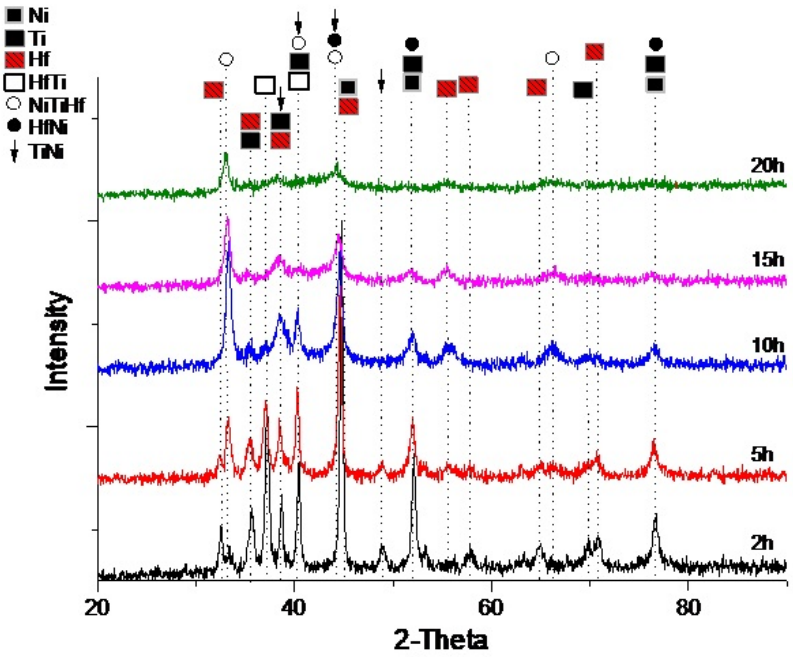


Figure 31. XRD of ball-milled NiTiHf powders [33].

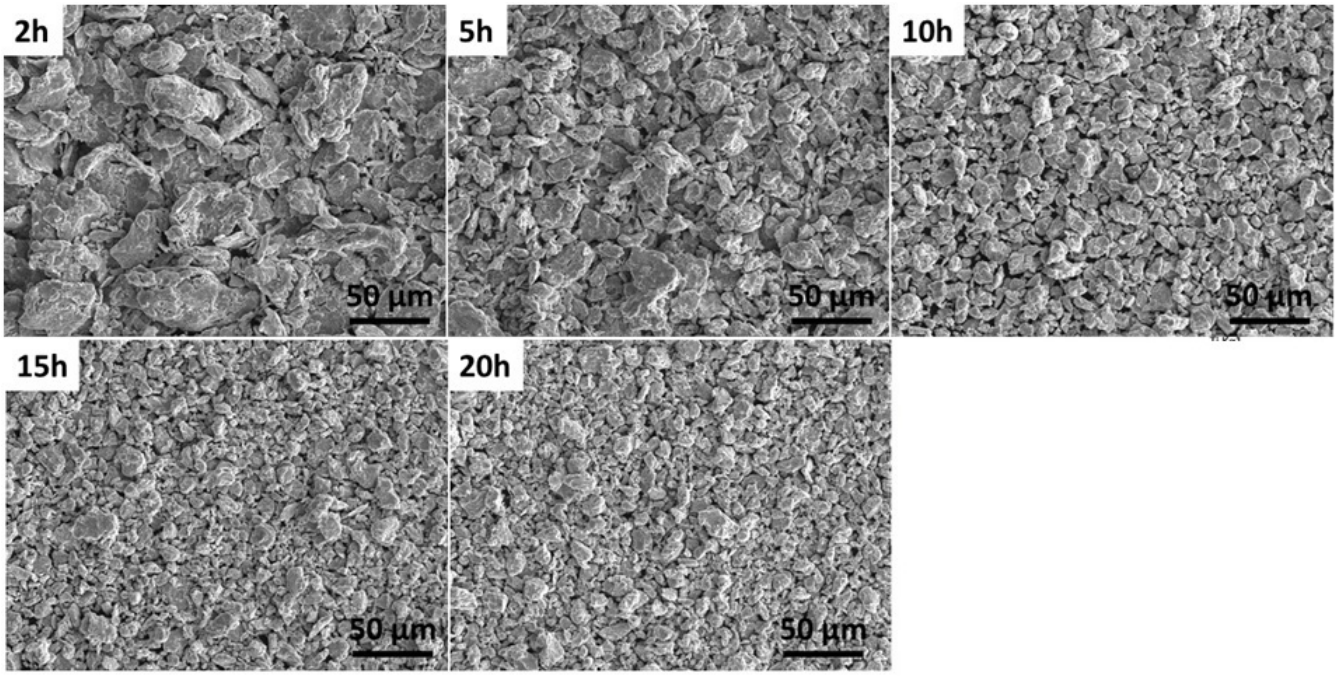


Figure 32. SEM and EDS analysis of ball-milled NiTiHf powders [33].

Initially, Shashanka et al. [33] investigated the electrocatalytic properties of NiTiHf-MCPE and found no remarkable increase in the current response; therefore, they electropolymerized the MCPE with methyl orange and studied their electrocatalytic properties in determining dopamine. After the process of electropolymerization, their current response increased from 40 to around 54 µA. Figure 33a shows the electropolymerized voltammograms after electropolymerized NiTiHf-MCPE with 1 mM methyl orange (MO) at a pH of 7 in 0.2 M phosphate buffer solution (PBS). For up to 20 cycles, the polymerization was carried out at a scan rate of 0.1 V/s and a potential range of 0.3 V to 1.2 V, respectively. It was verified by the voltammograms that a linear increase in Ipa could be seen as the number of cycles increased from 1 to 20; this is because a methyl orange monomer forms a polymer. The polymerization process enhances the NiTiHf-modified electrode's surface area, reactive sites, selectivity, and sensitivity in addition to raising the oxidation peak current. Figure 33b shows the CVs of electrochemical redox reactions of dopamine in BCPE, NiTiHf-MCPE, and poly(MO)-NiTiHf-MCPE, respectively. From the figure, it is confirmed that the electropolymerized MCPE has shown a maximum current response than the other two electrodes. Later authors calculated the active surface areas of BCPE, NiTiHf-MCPE, and poly(MO)-NiTiHf-MCPE using the Nernst equation, and the values were found to be 0.044, 0.089, and 0.098 cm^2, respectively. This shows the importance of modification and electropolymerization of the electrodes [33].

Figure 33c represents the effect of pH on the redox reaction of dopamine using poly(MO)-NiTiHf-MCPE, and it confirms the shifting of Epa to higher values linearly with the increase in the pH from 5 to 7.5. This confirms the participation of protons during the electrochemical redox reaction of dopamine. The linear regression equation for this study is as follows: Ep(V) = 0.1812 − (0.0591) pH (V/pH) (R^2 = 0.9984).

This linear regression equation demonstrates that during the redox reaction of dopamine, the electron mobility is mostly dependent on H+ [121]. The obtained slope of 0.0591 V/pH is extremely near to the conventional value of 0.059 V/pH. This demonstrates that the redox reaction of dopamine involves the same number of protons and electrons, which is determined to be two electrons and two protons. Figure 33d shows the CV of dopamine at different scan rates from 0.025 to 0.4 V/s at poly(MO)-NiTiHf-MCPE. It shows

an increase in the IPA with the increase in scan rate. The possible electrochemical oxidation of dopamine on the surface of poly(MO)-NiTiHf-MCPE is shown in Figure 34. Authors have also studied the effect of interferents, repeatability, stability, and reproducibility of poly(MO)-NiTi–MCPE during the electrochemical redox reaction of dopamine and they have reported excellent results [33]. They have also determined dopamine and FA simultaneously using the same poly(MO)-NiTi–MCPE and concluded that this electrode could be a potential candidate to determine various bioactive molecules individually or simultaneously in real samples. Table 1 depicts the comparison of experimental results of different types of alloy-MCPE during the determination of various analytes.

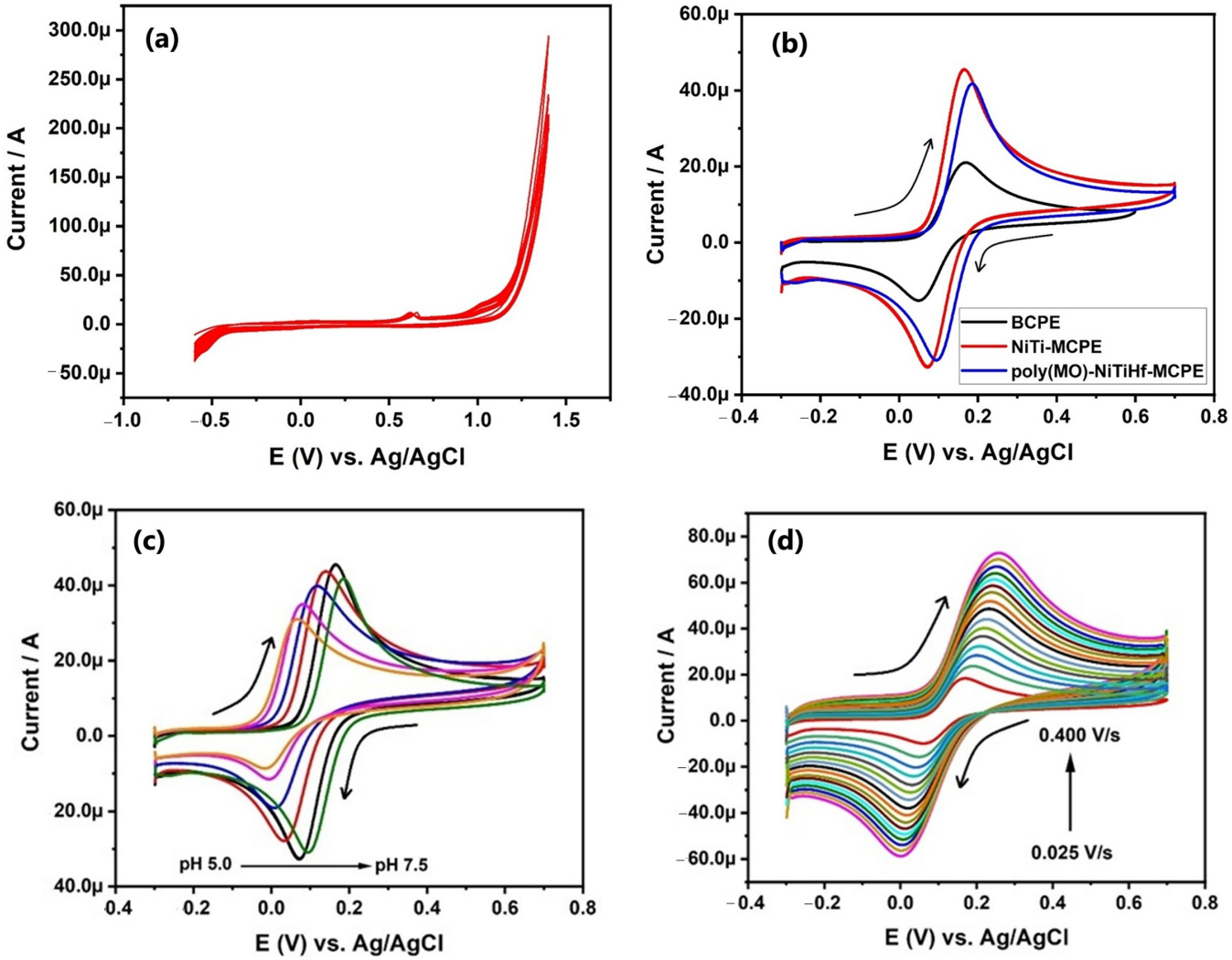


Figure 33. (**a**) CV after electropolymerized NiTiHf-MCPE with 1 mM methyl orange (MO) at a pH of 7 in 0.2 M phosphate buffer solution (PBS), (**b**) CV of electrochemical reaction of dopamine at BCPE, NiTi-MCPE, and poly(MO)-NiTiHf-MCPE, respectively; CVs of electrochemical redox reaction of dopamine using poly(MO)-NiTiHf-MCPE at different (**c**) PBS of pH, (**d**) scan rates [33].

Table 1. Comparison of experimental results of different types of alloy-MCPE during the determination of various analytes.

Modifiers Used	Electrochemical Technique	Analyte Determined	Important Findings	References
Fe-18Cr-13Ni (stainless steel)	CV	Folic Acid	Electrode reactions were adsorption controlled. Current sensitivity of 17.32 µA was recorded.	[29]

Table 1. *Cont.*

Modifiers Used	Electrochemical Technique	Analyte Determined	Important Findings	References
Duplex stainless steel	CV	Ascorbic Acid	The stainless steel showed good current sensitivity of 143.52 µA.	[25]
Duplex stainless steel	CV	Uric Acid	The stainless steel showed good current sensitivity of 19.36 µA.	[25]
Duplex stainless steel	CV	Dopamine	The stainless steel showed good current sensitivity of 25.61 µA.	[25]
Yttria dispersed Fe-18Cr-13Ni	CV	Ascorbic Acid	The stainless steel showed good current sensitivity of 370 mV.	[24]
Yttria dispersed duplex stainless steel	CV	Uric Acid	The stainless steel showed good current sensitivity of 31.01 µA.	[24]
Yttria dispersed duplex stainless steel	CV	Dopamine	The stainless steel showed good current sensitivity of 28.48 µA.	[24]
23Fe-21Cr-18Ni-20Ti-18Mn (HEA)	CV	Ascorbic Acid	For the concentration of 8 mg modifier, a maximum peak current of 104.07 µA was measured. For the high-entropy-alloy-modified carbon paste electrode and the bare carbon paste electrode, the active surface areas for the electron transfer process of ascorbic acid are calculated to be 0.0014 cm^2 and 0.0027 cm^2, respectively.	[30]
25Fe-19Cr-19Ni-18Ti-19Mn high-entropy alloy	CV	Methylene Blue	The anodic peak current of 508.4 µA was displayed by the 4 mg high-entropy-alloy-modified carbon paste electrode, while only 99.74 µA was displayed by the bare carbon paste electrode. This significant anodic peak current difference between the two different electrodes have demonstrated the value of the the modifier in enhancing the electrode sensor's sensitivity, robustness, and selectivity.	[32]
2507 super duplex stainless steel	CV	Ascorbic Acid	BCPE has shown an anodic peak current of 22.5 µA and 4 mg SDSS-MCPE has recorded 37.2 µA of anodic peak current during the electro-oxidation of 1 mM AA. LOD and LOQ were calculated to be 2.06 nM and 6.8 nM, respectively.	[26]
poly (methyl orange) shape memory alloy	CV	Dopamine	The calculated active surface area for BCPE, NiTiHf-MCPE, and the poly(MO)-NiTiHf-MCPE were found to be 0.044, 0.089, and 0.098 cm^2, respectively. LOD and LOQ were calculated to be 5.55 µM and 18.45 µM, respectively.	[33]

Table 1. *Cont.*

Modifiers Used	Electrochemical Technique	Analyte Determined	Important Findings	References
23Fe-21Cr-18Ni-20Ti-18Mn	CV	Methyl Orange	MO oxidizes at 700 mV. The calculated electrode surface area of BCPE and HEAMCPE was found to be 0.0546 and 0.4439 cm^2, respectively. The LOD obtained is 0.080 µM.	[31]

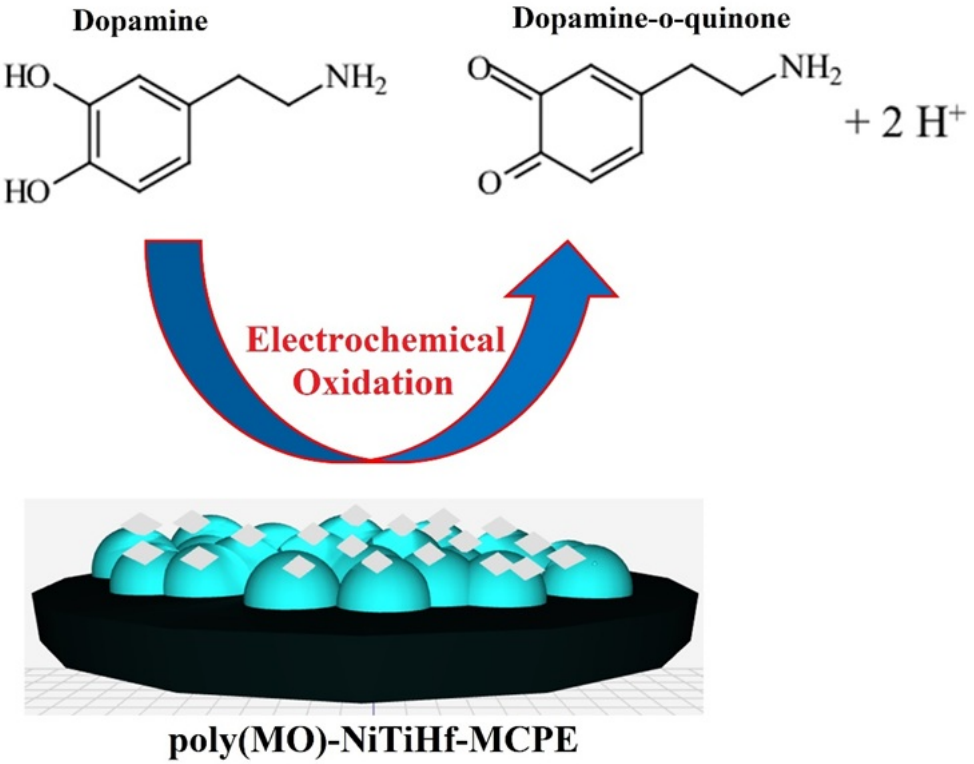


Figure 34. Possible electrochemical oxidation scheme of dopamine at poly(MO)-NiTiHf-MCPE [33].

8. Challenges and Future Perspectives

Although using nanostructured-alloy-modified CPEs for electrochemical sensing has several benefits, there are drawbacks as well:

- ➢ Reproducibility: Because of differences in how nanostructured alloys were prepared and how the nanoparticles were distributed in the past, it might be difficult to achieve similar performance across several sensors.
- ➢ Interference from Biological Matrices: Measurement accuracy may be impacted by the presence of interferents in complex biological samples, such as blood or urine. To reduce these interferences, sophisticated sensor designs and adjustments are required.
- ➢ Long-term Stability: Although nanostructured alloys are generally durable, oxidation and other causes may cause them to perform worse over time, which could compromise the sensors' long-term dependability.

By creating more reliable, repeatable electrode modification methods, improving sensor selectivity through sophisticated material design, and combining electrochemical sensors with portable devices for real-time applications, future research will probably concentrate on overcoming these obstacles.

9. Conclusions

Alloys are the perfect candidates for electrochemical sensing because of their exceptional conductivity and biocompatibility as electrocatalysts. Their catalytic qualities enable the oxidation or reduction of analytes at lower applied potentials, while their large surface area enables the effective adsorption of biomolecules. Selectivity and sensitivity towards particular analytes can be enhanced by the synergistic effects of alloys. Furthermore, the presence of nanostructured alloys on the electrode surface enhances the sensor's selectivity by enabling improved resolution of overlapping signals. These sensors are an important tool for environmental monitoring since they can identify minute levels of contaminants, harmful compounds, bioactive molecules, amino acids, and other substances in soil or water samples. The sensitivity of the sensor is raised by the significantly greater surface area that the nanoscale size of metal particles offers for the adsorption of target molecules. Because of their superior conductivity, these alloys—MCPE—produce more accurate and timely reactions by accelerating electron transport. They are also more durable and robust, which ensures that the sensors will perform effectively even under harsh circumstances and after extended use. Given the ongoing advancements in material science and sensor design, these modified electrodes are anticipated to play a key role in the development of next-generation diagnostic tools and environmental monitoring systems.

Author Contributions: Conceptualization, S.R. and V.A.; methodology, S.R. and R.S.M.; validation, Y.C. and G.R.C.; formal analysis, S.R. and R.S.M.; investigation, E.A. and V.A.; data curation, Y.C. and G.R.C.; writing—original draft preparation, S.R. and R.S.M.; writing—review and editing, S.R.; visualization, E.A., V.A. and Y.C.; supervision, S.R. All authors have read and agreed to the published version of the manuscript.

Funding: This research received no external funding.

Institutional Review Board Statement: Not applicable.

Informed Consent Statement: Not applicable.

Data Availability Statement: No new data were created or analyzed in this study. Data sharing is not applicable to this article.

Conflicts of Interest: The authors declare no conflicts of interest.

References

1. Yamaguchi, H.; Miyazaki, M. Enzyme-Immobilized Microfluidic Devices for Biomolecule Detection. *TrAC Trends Anal. Chem.* **2022**, *159*, 116908. [CrossRef]
2. Ziani, I.; Bouakline, H.; Guerraf, A.E.; Bachiri, A.E.; Fauconnier, N.M.-L.; Sher, F. Integrating AI and Advanced Spectroscopic Techniques for Precision Food Safety and Quality Control. *Trends Food Sci. Technol.* **2024**, *156*, 104850. [CrossRef]
3. Manjunatha, J.G. *Advances in Surfactant Biosensor and Sensor Technologies*; Elsevier: Amsterdam, The Netherlands, 2024. [CrossRef]
4. Charithra, M.M.; Manjunatha, J.G.G.; Hareesha, N.; Prinith, S.N.; Ravishankar, D.K.; Arpitha, H.J. An Overview of Recent Development in Carbon-Based Sensors for Neurotransmitter Detection. *Comb. Chem. High Throughput Screen.* **2023**, *26*, 2614–2624. [CrossRef] [PubMed]
5. Hareesha, N.; Manjunatha, J.G.; Girish, T.; ALOthman, Z.A. Analysis of Catechol as an Environmental Pollutant Based on Electropolymerised Methyl Orange Modified Carbon Paste Sensor. *Int. J. Environ. Anal. Chem.* **2023**, *104*, 9186–9198. [CrossRef]
6. Senthilkumar, N.; Babu, K.J.; Kumar, G.G.; Kim, A.R.; Yoo, D.J. Flexible Electrospun PVDF-HFP/NI/CO Membranes for Efficient and Highly Selective Enzyme Free Glucose Detection. *Ind. Eng. Chem. Res.* **2014**, *53*, 10347–10357. [CrossRef]
7. Tamilarasi, S.; Kumar, R.S.; Cho, K.-B.; Kim, C.-J.; Yoo, D.J. High-Performance Electrochemical Detection of Glucose in Human Blood Serum Using a Hierarchical NiO2 Nanostructure Supported on Phosphorus Doped Graphene. *Mater. Today Chem.* **2023**, *34*, 101765. [CrossRef]
8. Nadar, N.R.; Deepak, J.; Sharma, S.C.; Krushna, B.R.R.; Puneeth, N.; Sowjanya, R.; Varalakshmi, V.S.; Sahu, S.; Sargunam, B.; Nagabhushana, H.; et al. Graphene Oxide Based Gd_2O_3:Eu^{3+} Nanocomposites: A Multifaceted Approach to Advanced Energy Storage and Bio Sensing Applications. *Inorg. Chem. Commun.* **2024**, *165*, 112515. [CrossRef]

9. Vaibhav, N.; Swamy, B.E.K.; Manjunatha, L.S.; Manjunatha, K.G.; Sharma, S.C. Electrochemical Determination of Uric Acid in Presence of FA Using Synthesized Cobalt Oxide Modified Carbon Paste Electrode. *Inorg. Chem. Commun.* **2024**, *165*, 112469. [CrossRef]
10. Nadar, N.R.; Deepak, J.; Sharma, S.C.; Krushna, B.R.R.; Puneeth, N.; Sowjanya, R.; Varalakshmi, V.S.; Sahu, S.; Sargunam, B.; Nagabhushana, H.; et al. Synergistic Doping Strategies Boosting Electrochemical Performance: GO-Y_2O_3: Eu^{3+}/Li^+ Nanocomposites for Supercapacitor and Biosensor Applications. *Inorg. Chem. Commun.* **2024**, *164*, 112397. [CrossRef]
11. Atta, N.F.; Gawad, S.A.A.; Galal, A.; Razik, A.A.; El-Gohary, A.R. Efficient Electrochemical Sensor for Determination of H_2O_2 in Human Serum Based on Nano Iron-nickel Alloy/Carbon Nanotubes/Ionic Liquid Crystal Composite. *J. Electroanal. Chem.* **2020**, *881*, 114953. [CrossRef]
12. Hernández-Saravia, L.P.; Martinez, T.; Llanos, J.; Bertotti, M. A Cu-NPG/SPE Sensor for Non-Enzymatic and Non-Invasive Electrochemical Glucose Detection. *Microchem. J.* **2020**, *160*, 105629. [CrossRef]
13. Hajmalek, S.; Jahani, S.; Foroughi, M.M. Simultaneous Voltammetric Determination of Tramadol and Paracetamol Exploiting Glassy Carbon Electrode Modified with $FeNi_3$ Nanoalloy in Biological and Pharmaceutical Media. *ChemistrySelect* **2021**, *6*, 8797–8808. [CrossRef]
14. Halfadji, A.; Naous, M.; Rajendrachari, S.; Ceylan, Y.; Ceylan, K.B.; Shekar, P.V.R. Effective Investigation of Electro-Catalytic, Photocatalytic, and Antimicrobial Properties of Porous CuO Nanoparticles Green Synthesized Using Leaves of Cupressocyparis Leylandii. *J. Mol. Struct.* **2023**, *1301*, 137318. [CrossRef]
15. Halfadji, A.; Naous, M.; Kharroubi, K.N.; Belmehdi, F.E.Z.; Rajendrachari, S. An Ultrasonic-Assisted Synthesis, Characterization, and Application of Nano-Fe_3O_4/TiO_2 as Nano-Catalyst for the Removal of Organic Dye by Like-Photo-Fenton Reactions. *Inorg. Chem. Commun.* **2023**, *158*, 111686. [CrossRef]
16. Halfadji, A.; Chougui, A.; Djeradi, R.; Ouabad, F.Z.; Aoudia, H.; Rajendrachari, S. TiO_2-Decorated by Nano-γ-Fe_2O_3 as a Catalyst for Efficient Photocatalytic Degradation of Orange G Dye under Eco-Friendly White LED Irradiation. *ACS Omega* **2023**, *8*, 39907–39916. [CrossRef]
17. Rajendrachari Shashanka, B.N.; M Avar, B.S.P.; Kumar, R.M.; Baek, K.H. Assessing the Food Quality Using Carbon Nanomaterial Based Electrodes by Voltammetric Techniques. *Biosensors* **2022**, *12*, 1173. [CrossRef]
18. Rajendrachari, S.; Jayaprakash, G.K.; Pandith, A.; Karaoglanli, A.C.; Uzun, O. Electrocatalytic Investigation by Improving the Charge Kinetics between Carbon Electrodes and Dopamine Using Bio-Synthesized CuO Nanoparticles. *Catalysts* **2022**, *12*, 994. [CrossRef]
19. Mahale, R.S.; Shamanth, V.K.; Hemanth, K.; Shashanka, R.; Sharath, P.C.; Sreekanth, N.V. Electrochemical Sensor Applications of Nanoparticle Modified Carbon Paste Electrodes to Detect Various Neurotransmitters: A Review. *Appl. Mech. Mater.* **2022**, *908*, 69–88. [CrossRef]
20. Shashanka, R.; Jayaprakash, G.K.; BG, P.; Kumar, M.; Swamy, B.E.K. Electrocatalytic Determination of AA Using a Green Synthesised Magnetite Nano-Flake Modified Carbon Paste Electrode by Cyclic Voltammetric Method. *Mater. Res. Innov.* **2021**, *26*, 229–239. [CrossRef]
21. Pavitra, V.; Praveen, B.M.; Nagaraju, G.; Shashanka, R. Energy Storage, Photocatalytic and Electrochemical Nitrite Sensing of Ultrasound-Assisted Stable TA_2O_5 Nanoparticles. *Top. Catal.* **2022**. [CrossRef]
22. Rajendrachari, S.; Ramakrishna, D. Functionalized Nanomaterial-Based Electrochemical Sensors: ASensitive Sensor Platform. In *Elsevier eBooks*; Woodhead Publishing: Cambridge, UK, 2022; pp. 3–25.
23. Rajendrachari, S.; Taslimi, P.; Karaoglanli, A.C.; Uzun, O.; Alp, E.; Jayaprakash, G.K. Photocatalytic Degradation of Rhodamine B (RhB) Dye in Waste Water and Enzymatic Inhibition Study Using Cauliflower Shaped ZnO Nanoparticles Synthesized by a Novel One-Pot Green Synthesis Method. *Arab. J. Chem.* **2021**, *14*, 103180. [CrossRef]
24. Shashanka, R.; Chaira, D.; Swamy, B.E.K. Fabrication of yttria dispersed duplex stainless steel electrode to determine dopamine, ascorbic and uric acid electrochemically by using cyclic voltammetry. *Int. J. Sci. Eng. Res.* **2016**, *7*, 1275–1285.
25. Shashanka, R.; Chaira, D.; Swamy, B.E.K. Electrochemical investigation of duplex stainless steel at carbon paste electrode and its application to the detection of dopamine, ascorbic and uric acid. *Int. J. Sci. Eng. Res.* **2015**, *6*, 1863–1871.
26. Mahale, R.S.; Vasanth, S.; Chikkegouda, S.P.; Rajendrachari, S.; Narsimhachary, D.; Basavegowda, N. Electrochemical Determination of AA by Mechanically Alloyed Super Duplex Stainless Steel Powders. *Metals* **2023**, *13*, 1430. [CrossRef]
27. Mahale, R.S.; Rajashekar, V.; Vasanth, S.; Chikkegowda, S.P.; Rajendrachari, S.; Mahesh, V. Fabrication of Mechanically Alloyed Super Duplex Stainless Steel Powder-Modified Carbon Paste Electrode for the Determination of MBby the Cyclic Voltammetry Technique. *ACS Omega* **2024**, *9*, 10660–10670. [CrossRef]
28. Rajendrachari, S.; Vinaykumar, R.; Katti, R.; Koujalagi, B.G.; Jayaprakash, G.K.; Ramkumar, R. Cyclic Voltammetric Determination of Rhodamine B Dye Using a Gas-Atomized Duplex Stainless Steel Powder-Modified Carbon Paste Electrode. *Top. Catal.* **2024**. [CrossRef]

29. Shashanka, R.; Chaira, D.; Swamy, B.E.K. Electrocatalytic Response of Duplex and Yittria Dispersed Duplex Stainless Steel Modified Carbon Paste Electrode in Detecting FA Using Cyclic Voltammetry. *Int. J. Electrochem. Sci.* **2015**, *10*, 5586–5598. [CrossRef]
30. Rajendrachari, S.; Adimule, V.; Gulen, M.; Khosravi, F.; Somashekharappa, K.K. Synthesis and Characterization of High Entropy Alloy 23Fe-21Cr-18Ni-20Ti-18Mn for Electrochemical Sensor Applications. *Materials* **2022**, *15*, 7591. [CrossRef]
31. Rajendrachari, S.; Mahale, R.S.; Adimule, V.; Gulen, M.; Mahesh, V.; Basavegowda, N. Fabrication of Mechanically Alloyed High Entropy Alloys (20-Fe-20Cr-20Ni-20Mn-20Ti) Modified Carbon Paste Electrode Sensor for the Cyclic Voltammetric Determination of Methyl Orange. *Inorg. Chem. Commun.* **2024**, *164*, 112428. [CrossRef]
32. Rajendrachari, S.; Adimule, V.M.; Jayaprakash, G.K.; Pandith, A. Electrochemical Oxidation of MB Dye in Wastewater Using Mechanically Alloyed High Entropy Alloy Modified Carbon Paste Electrode Using Cyclic Voltammetry. *Mater. Res. Express* **2023**, *10*, 054003. [CrossRef]
33. Rajendrachari, S.; Altaş, E.; Erdogan, A.; Küçük, Y.; Gök, M.S.; Khosravi, F. Electrochemical Determination of Dopamine by Poly (Methyl Orange) Shape Memory Alloy Modified Carbon Paste Electrode. *Inorg. Chem. Commun.* **2024**, *167*, 112826. [CrossRef]
34. Suryanarayana, C. Mechanical Alloying and Milling. *Prog. Mater. Sci.* **2001**, *46*, 1–184. [CrossRef]
35. Suryanarayana, C. Nanocrystalline Materials. *Int. Mater. Rev.* **1995**, *40*, 41–64. [CrossRef]
36. Suryanarayana, C.; Ivanov, E.; Boldyrev, V.V. The Science and Technology of Mechanical Alloying. *Mater. Sci. Eng. A* **2001**, *304–306*, 151–158. [CrossRef]
37. Prabhu, B.; Suryanarayana, C.; An, L.; Vaidyanathan, R. Synthesis and Characterization of High Volume Fraction Al–Al_2O_3 Nanocomposite Powders by High-Energy Milling. *Mater. Sci. Eng. A* **2006**, *425*, 192–200. [CrossRef]
38. Suryanarayana, C. Structure and Properties of Nanocrystalline Materials. *Bull. Mater. Sci.* **1994**, *17*, 307–346. [CrossRef]
39. Suryanarayana, C. Mechanical Alloying: A Novel Technique to Synthesize Advanced Materials. *Research* **2019**, *2019*, 4219812. [CrossRef]
40. Shashanka, R.; Chaira, D. Optimization of Milling Parameters for the Synthesis of Nano-Structured Duplex and Ferritic Stainless Steel Powders by High Energy Planetary Milling. *Powder Technol.* **2015**, *278*, 35–45. [CrossRef]
41. Chaira, D. Development of Nano-Structured Duplex and Ferritic Stainless Steels by Pulverisette Planetary Milling Followed by Pressureless Sintering. *Mater. Charact.* **2014**, *99*, 220–229. [CrossRef]
42. Chaira, D. Phase Transformation and Microstructure Study of Nano-Structured Austenitic and Ferritic Stainless Steel Powders Prepared by Planetary Milling. *Powder Technol.* **2014**, *259*, 125–136. [CrossRef]
43. Hocevar, S.; Ogorevc, B. Preparation and Characterization of Carbon Paste Micro-Electrode Based on Carbon Nano-Particles. *Talanta* **2007**, *74*, 405–411. [CrossRef] [PubMed]
44. Apetrei, C.; Apetrei, I.M.; De Saja, J.A.; Rodriguez-Mendez, M.L. Carbon Paste Electrodes Made from Different Carbonaceous Materials: Application in the Study of Antioxidants. *Sensors* **2011**, *11*, 1328–1344. [CrossRef] [PubMed]
45. Abbaspour, A. Chemically Modified Carbon Paste Electrode for Determination of Copper(II) by Potentiometric Method. *Talanta* **2002**, *56*, 91–96. [CrossRef] [PubMed]
46. Koirala, K.; Santos, J.H.; Tan, A.L.; Ali, M.A.; Mirza, A.H. Chemically Modified Carbon Paste Electrode for the Detection of Lead, Cadmium and Zinc Ions. *Sens. Rev.* **2016**, *36*, 339–346. [CrossRef]
47. Nesakumar, N.; Berchmans, S.; Alwarappan, S. Chemically Modified Carbon Based Electrodes for the Detection of Reduced Glutathione. *Sens. Actuators B Chem.* **2018**, *264*, 448–466. [CrossRef]
48. Ghassab, N.; Soleymanpour, A.; Shafaatian, B. Development of an Ultrasensitive Chemically Modified Carbon Paste Electrode for Selective Determination Trace Amount of Sulfate Ion. *Measurement* **2022**, *205*, 112231. [CrossRef]
49. Soleymanpour, A.; Shafaatian, B.; Mirfakhraei, H.S.; Rezaeifard, A. Development of a New Chemically Modified Carbon Paste Electrode for Selective Determination of Urinary and Serum Oxalate Concentration. *Talanta* **2013**, *116*, 427–433. [CrossRef]
50. Wang, H.; Qian, D.; Xiao, X.; Deng, C.; Liao, L.; Deng, J.; Lin, Y.-W. Preparation and Application of a Carbon Paste Electrode Modified with Multi-Walled Carbon Nanotubes and Boron-Embedded Molecularly Imprinted Composite Membranes. *Bioelectrochemistry* **2018**, *121*, 115–124. [CrossRef]
51. Hamidi, H.; Shams, E.; Yadollahi, B.; Esfahani, F.K. Fabrication of Bulk-Modified Carbon Paste Electrode Containing α-PW12O403−Polyanion Supported on Modified Silica Gel: Preparation, Electrochemistry and Electrocatalysis. *Talanta* **2007**, *74*, 909–914. [CrossRef]
52. Ali, T.A.; Mohamed, G.G. Determination of Mn(II) Ion by a Modified Carbon Paste Electrode Based on Multi-Walled Carbon Nanotubes (MWCNTs) in Different Water Samples. *Sens. Actuators B Chem.* **2014**, *202*, 699–707. [CrossRef]
53. Zaib, M.; Athar, M.M. Electrochemical Evaluation of Biologically Modified Carbon Paste Electrode with Cyclic Voltammetric Technique. *Port. Electrochim. Acta* **2019**, *37*, 285–294. [CrossRef]
54. Francis, R.; Byrne, G. Duplex Stainless Steels—Alloys for the 21st Century. *Metals* **2021**, *11*, 836. [CrossRef]
55. Straße, A.; Gumenyuk, A.; Rethmeier, M. Study on Duplex Stainless Steel Powder Compositions for the Coating of Thick Plates for Laser Beam Welding. *Adv. Eng. Mater.* **2022**, *24*, 2101327. [CrossRef]

56. Pezzato, L.; Calliari, I. Advances in Duplex Stainless Steels. *Materials* **2022**, *15*, 7132. [CrossRef]
57. Omiogbemi, I.M.-B.; Yawas, D.S.; Das, A.; Afolayan, M.O.; Dauda, E.T.; Kumar, R.; Gorja, S.R.; Chowdhury, S.G. Mechanical Properties and Corrosion Behaviour of Duplex Stainless Steel Weldment Using Novel Electrodes. *Sci. Rep.* **2022**, *12*, 22405. [CrossRef]
58. Alvarez-Armas, I. Duplex Stainless Steels: Brief History and Some Recent Alloys. *Recent Pat. Mech. Eng.* **2008**, *1*, 51–57. [CrossRef]
59. Han, Y.; Liu, Z.-H.; Wu, C.-B.; Zhao, Y.; Zu, G.-Q.; Zhu, W.-W.; Ran, X. A Short Review on the Role of Alloying Elements in Duplex Stainless Steels. *Tungsten* **2022**, *5*, 419–439. [CrossRef]
60. Besharatloo, H.; Carpio, M.; Cabrera, J.-M.; Mateo, A.M.; Fargas, G.; Wheeler, J.M.; Roa, J.J.; Llanes, L. Novel Mechanical Characterization of Austenite and Ferrite Phases within Duplex Stainless Steel. *Metals* **2020**, *10*, 1352. [CrossRef]
61. Duplex Stainless Steels. In *ASM International eBooks*; ASM: Almere, The Netherlands, 2008; pp. 91–107.
62. Olguín, H.J.; Guzmán, D.C.; García, E.H.; Mejía, G.B. The Role of Dopamine and Its Dysfunction as a Consequence of Oxidative Stress. *Oxidative Med. Cell. Longev.* **2015**, *2016*, 9730467. [CrossRef]
63. Speranza, L.; Di Porzio, U.; Viggiano, D.; De Donato, A.; Volpicelli, F. Dopamine: The Neuromodulator of Long-Term Synaptic Plasticity, Reward and Movement Control. *Cells* **2021**, *10*, 735. [CrossRef]
64. Franco, R.; Reyes-Resina, I.; Navarro, G. Dopamine in Health and Disease: Much More than a Neurotransmitter. *Biomedicines* **2021**, *9*, 109. [CrossRef] [PubMed]
65. Tian, Y. The Role of Dopamine Neurotransmitters in Neurological Diseases: New Sight. *Int. J. Mol. Sci.* **2024**, *25*, 7529. [CrossRef] [PubMed]
66. Meder, D.; Herz, D.M.; Rowe, J.B.; Lehéricy, S.; Siebner, H.R. The Role of Dopamine in the Brain-Lessons Learned from Parkinson's Disease. *NeuroImage* **2018**, *190*, 79–93. [CrossRef] [PubMed]
67. Latif, S.; Jahangeer, M.; Razia, D.M.; Ashiq, M.; Ghaffar, A.; Akram, M.; Allam, A.E.; Bouyahya, A.; Garipova, L.; Shariati, M.A.; et al. Dopamine in Parkinson's Disease. *Clin. Chim. Acta* **2021**, *522*, 114–126. [CrossRef]
68. Cramb, K.M.L.; Beccano-Kelly, D.; Cragg, S.J.; Wade-Martins, R. Impaired Dopamine Release in Parkinson's Disease. *Brain* **2023**, *146*, 3117–3132. [CrossRef]
69. Falamaş, A.; Petran, A.; Hada, A.-M.; Bende, A. Dopamine Photochemical Behaviour under UV Irradiation. *Int. J. Mol. Sci.* **2022**, *23*, 5483. [CrossRef]
70. Amare, M. Electrochemical Determination of AA in Pharmaceutical Tablets Using Carbon Paste Electrode. *Org. Med. Chem. Int. J.* **2019**, *8*, 124–132. [CrossRef]
71. Hamam, A.; Maiza, M. Voltammetric Determination of AA Using Cu Foil Electrode. *Int. J. Electrochem. Sci.* **2021**, *16*, 210426. [CrossRef]
72. Alemu, T.; Zelalem, B.; Amare, N. Voltammetric Determination of AA Content in Cabbage Using Anthraquinone Modified Carbon Paste Electrode. *J. Chem.* **2022**, *2022*, 7154170. [CrossRef]
73. Parkook, F.; Shahvandi, S.K.; Ghaedi, M.; Javadian, H.; Parkook, A. Determination of AA in Biological Samples Using an Electrochemical Sensor Modified with Au-Cu2O/MWCNTs Nanocomposite. *Diam. Relat. Mater.* **2024**, *144*, 110954. [CrossRef]
74. Rončević, I.Š.; Skroza, D.; Vrca, I.; Kondža, A.M.; Vladislavić, N. Development and Optimization of Electrochemical Method for Determination of Vitamin C. *Chemosensors* **2022**, *10*, 283. [CrossRef]
75. Gülen, M.; Taş, R.; Dünya, H.; Rajendrachari, S. Enlargement of the Surface Area of High-Entropy Alloys with Acid Treatment as Positive Electrode for High Specific Capacitance Supercapacitors. *ChemistryOpen* **2025**. [CrossRef] [PubMed]
76. Skrovankova, S.; Mlcek, J.; Sochor, J.; Baron, M.; Kynicky, J.; Jurikova, T. Determination of AA by Electrochemical Techniques and Other Methods. *Int. J. Electrochem. Sci.* **2015**, *10*, 2421–2431. [CrossRef]
77. Thbayh, D.K.; Reizer, E.; Kahaly, M.U.; Viskolcz, B.; Fiser, B. Antioxidant Potential of Santowhite as Synthetic and AA as Natural Polymer Additives. *Polymers* **2022**, *14*, 3518. [CrossRef]
78. Ramkumar, R.; Veerakumar, P.; Rajendrachari, S.; Dhakal, G.; Yun, J.; Shim, J.-J.; Kim, W.K. Copper Aerogel Frameworks—Electrochemical Detection of Dopamine and Catalytic Reduction of 4-Nitrophenol. *Microchem. J.* **2024**, *208*, 112486. [CrossRef]
79. Khan, I.; Saeed, K.; Zekker, I.; Zhang, B.; Hendi, A.H.; Ahmad, A.; Ahmad, S.; Zada, N.; Ahmad, H.; Shah, L.A.; et al. Review on Methylene Blue: Its Properties, Uses, Toxicity and Photodegradation. *Water* **2022**, *14*, 242. [CrossRef]
80. Bužga, M.; Machytka, E.; Dvořáčková, E.; Švagera, Z.; Stejskal, D.; Máca, J.; Král, J. Methylene Blue: A Controversial Diagnostic Acid and Medication? *Toxicol. Res.* **2022**, *11*, 711–717. [CrossRef]
81. Taldaev, A.; Terekhov, R.; Nikitin, I.; Melnik, E.; Kuzina, V.; Klochko, M.; Reshetov, I.; Shiryaev, A.; Loschenov, V.; Ramenskaya, G. MBin Anticancer Photodynamic Therapy: Systematic Review of Preclinical Studies. *Front. Pharmacol.* **2023**, *14*, 1264961. [CrossRef]
82. Xiong, Z.-M.; O'Donovan, M.; Sun, L.; Choi, J.Y.; Ren, M.; Cao, K. Anti-Aging Potentials of MBfor Human Skin Longevity. *Sci. Rep.* **2017**, *7*, 2475. [CrossRef]
83. Vasiljevic, Z.Z.; Dojcinovic, M.P.; Vujancevic, J.D.; Jankovic-Castvan, I.; Ognjanovic, M.; Tadic, N.B.; Stojadinovic, S.; Brankovic, G.O.; Nikolic, M.V. Photocatalytic Degradation of MBunder Natural Sunlight Using Iron Titanate Nanoparticles Prepared by a Modified Sol–Gel Method. *R. Soc. Open Sci.* **2020**, *7*, 200708. [CrossRef]

84. Fito, J.; Abewaa, M.; Mengistu, A.; Angassa, K.; Ambaye, A.D.; Moyo, W.; Nkambule, T. Adsorption of MBfrom Textile Industrial Wastewater Using Activated Carbon Developed from Rumex Abyssinicus Plant. *Sci. Rep.* **2023**, *13*, 5427. [CrossRef] [PubMed]
85. Oladoye, P.O.; Ajiboye, T.O.; Omotola, E.O.; Oyewola, O.J. MBDye: Toxicity and Potential Elimination Technology from Wastewater. *Results Eng.* **2022**, *16*, 100678. [CrossRef]
86. Modi, S.; Yadav, V.K.; Gacem, A.; Ali, I.H.; Dave, D.; Khan, S.H.; Yadav, K.K.; Rather, S.-U.; Ahn, Y.; Son, C.T.; et al. Recent and Emerging Trends in Remediation of MBDye from Wastewater by Using Zinc Oxide Nanoparticles. *Water* **2022**, *14*, 1749. [CrossRef]
87. Mulushewa, Z.; Dinbore, W.T.; Ayele, Y. Removal of MBfrom Textile Waste Water Using Kaolin and Zeolite-x Synthesized from Ethiopian Kaolin. *Environ. Anal. Health Toxicol.* **2021**, *36*, e2021007. [CrossRef]
88. Vutskits, L.; Briner, A.; Klauser, P.; Gascon, E.; Dayer, A.G.; Kiss, J.Z.; Muller, D.; Licker, M.J.; Morel, D.R. Adverse Effects of MBon the Central Nervous System. *Anesthesiology* **2008**, *108*, 684–692. [CrossRef]
89. Albert, M.; Lessin, M.S.; Gilchrist, B.F. Methylene Blue: Dangerous Dye for Neonates. *J. Pediatr. Surg.* **2003**, *38*, 1244–1245. [CrossRef]
90. Auerbach, S.S.; Bristol, D.W.; Peckham, J.C.; Travlos, G.S.; Hébert, C.D.; Chhabra, R.S. Toxicity and Carcinogenicity Studies of MBTrihydrate in F344N Rats and B6C3F1 Mice. *Food Chem. Toxicol.* **2009**, *48*, 169–177. [CrossRef]
91. Silva, M.; Caro, V.; Guzmán, C.; Perry, G.; Areche, C.; Cornejo, A. α-Synuclein and Tau, Two Targets for Dementia. *Stud. Nat. Prod. Chem.* **2020**, *67*, 1–25.
92. Saigl, Z.M. Various Adsorbents for Removal of Rhodamine B Dye: A Review. *Indones. J. Chem.* **2021**, *21*, 1039. [CrossRef]
93. Sharma, J.; Sharma, S.; Bhatt, U.; Soni, V. Toxic Effects of Rhodamine B on Antioxidant System and Photosynthesis of Hydrilla Verticillata. *J. Hazard. Mater. Lett.* **2022**, *3*, 100069. [CrossRef]
94. Al-Buriahi, A.K.; Al-Gheethi, A.A.; Kumar, P.S.; Mohamed, R.M.S.R.; Yusof, H.; Alshalif, A.F.; Khalifa, N.A. Elimination of Rhodamine B from Textile Wastewater Using Nanoparticle Photocatalysts: A Review for Sustainable Approaches. *Chemosphere* **2021**, *287*, 132162. [CrossRef] [PubMed]
95. Khubiev, O.M.; Egorov, A.R.; Semenkova, D.I.; Salokho, D.S.; Golubev, R.A.; Sikaona, N.D.; Lobanov, N.N.; Kritchenkov, I.S.; Tskhovrebov, A.G.; Kirichuk, A.A.; et al. Rhodamine B-Containing Chitosan-Based Films: Preparation, Luminescent, Antibacterial, and Antioxidant Properties. *Polymers* **2024**, *16*, 755. [CrossRef] [PubMed]
96. Chadelaud, T.; Zeghioud, H.; De La Garza, A.R.; Fuerte, O.; Benítez-Rico, A.; Revel, M.; Chávez-Miyauchi, T.E.; Djelal, H. Comparative Study of Rhodamine B Treatment: Assessing of Efficiency Processes and Ecotoxicity of By-Products. *Processes* **2023**, *11*, 2671. [CrossRef]
97. Kapoor, K.; Bala, M.; Choudhary, P.; Mridula, D.; Singh, R.K. Development of Method for Detection of Rhodamine B Dye in Chilli Powder (*Capsicum annuum* L.). *Asian J. Dairy Food Res.* **2022**, *43*, 539–543. [CrossRef]
98. Vizuete, G.; Santana-Romo, F.; Almeida-Naranjo, C.E. Virtual Screening of Fluorescent Heterocyclic Molecules and Advanced Oxidation Degradation of Rhodamine B in Synthetic Solutions. *Water* **2024**, *16*, 2141. [CrossRef]
99. Smith, A.D.; Kim, Y.-I.; Refsum, H. Is Folic Acid Good for Everyone? *Am. J. Clin. Nutr.* **2008**, *87*, 517–533. [CrossRef]
100. Shulpekova, Y.; Nechaev, V.; Kardasheva, S.; Sedova, A.; Kurbatova, A.; Bueverova, E.; Kopylov, A.; Malsagova, K.; Dlamini, J.C.; Ivashkin, V. The Concept of FA in Health and Disease. *Molecules* **2021**, *26*, 3731. [CrossRef]
101. Pamunuwa, G.; Nilakshi, H.; Rajapaksha, G.; Shakoor, F.; Karunaratne, D.N. Sensory and Physicochemical Properties and Stability of FA in a Pineapple Ready-to-Serve Beverage Fortified with Encapsulated FA. *J. Food Qual.* **2021**, *2021*, 9913884. [CrossRef]
102. Pertiwi, H.; Mahendra, M.Y.N.; Kamaludeen, J. FA: Sources, Chemistry, Absorption, Metabolism, Beneficial Effects on Poultry Performance and Health. *Vet. Med. Int.* **2022**, *2022*, 2163756. [CrossRef]
103. Ismail, S.; Eljazzar, S.; Ganji, V. Intended and Unintended Benefits of FA Fortification—A Narrative Review. *Foods* **2023**, *12*, 1612. [CrossRef]
104. Ajeigbe, K.; Aibangbee, K.; Saeed, S.; Ajeigbe, O.; Onifade, A. FA Protects and Heals Gastric Mucosa: Role of Acid Output, Inflammatory Cytokines, Angiogenic and Growth Factors. *J. Basic Appl. Zool.* **2022**, *83*, 15. [CrossRef]
105. Pérez-Carreón, K.; Martínez, L.M.; Videa, M.; Cruz-Angeles, J.; Gómez, J.; Ramírez, E. Effect of Basic Amino Acids on FA Solubility. *Pharmaceutics* **2023**, *15*, 2544. [CrossRef] [PubMed]
106. Krishna, S.A.; Noble, N.; Radhika, N.; Saleh, B. A Comprehensive Review on Advances in High Entropy Alloys: Fabrication and Surface Modification Methods, Properties, Applications, and Future Prospects. *J. Manuf. Process.* **2023**, *109*, 583–606. [CrossRef]
107. Kumar, A.; Singh, A.; Suhane, A. Mechanically Alloyed High Entropy Alloys: Existing Challenges and Opportunities. *J. Mater. Res. Technol.* **2022**, *17*, 2431–2456. [CrossRef]
108. Xie, X.; Li, N.; Liu, W.; Huang, S.; He, X.; Yu, Q.; Xiong, H.; Wang, E.; Hou, X. Research Progress of Refractory High Entropy Alloys: A Review. *Chin. J. Mech. Eng.* **2022**, *35*, 142. [CrossRef]
109. Wang, X.; Guo, W.; Fu, Y. High-Entropy Alloys: Emerging Materials for Advanced Functional Applications. *J. Mater. Chem. A* **2020**, *9*, 663–701. [CrossRef]

110. Rajendrachari, S. An Overview of High-Entropy Alloys Prepared by Mechanical Alloying Followed by the Characterization of Their Microstructure and Various Properties. *Alloys* **2022**, *1*, 116–132. [CrossRef]
111. Vaidya, M.; Muralikrishna, G.M.; Murty, B.S. High-Entropy Alloys by Mechanical Alloying: A Review. *J. Mater. Res.* **2019**, *34*, 664–686. [CrossRef]
112. Custodio, A.G.D.; Saha, G.C.; Aranas, C. Mechanical Alloying of AlCoCrFe and AlCoCrFeNi: Design and Experimental Evaluation of Medium- and High-Entropy Alloy Particles for Cold Spraying. *Powder Technol.* **2024**, *437*, 119556. [CrossRef]
113. Santiago-Andrades, L.; Vidal-Crespo, A.; Blázquez, J.S.; Ipus, J.J.; Conde, C.F. Mechanical Alloying as a Way to Produce Metastable Single-Phase High-Entropy Alloys beyond the Stability Criteria. *Nanomaterials* **2023**, *14*, 27. [CrossRef]
114. Kumar, A.; Singh, A.; Suhane, A. A Critical Review on Mechanically Alloyed High Entropy Alloys: Processing Challenges and Properties. *Mater. Res. Express* **2022**, *9*, 052001. [CrossRef]
115. Tsukamoto, H. Mechanical Behavior of Shape Memory Alloy Fiber Reinforced Aluminum Matrix Composites. *Mater. Today Commun.* **2021**, *29*, 102750. [CrossRef]
116. Balasubramanian, M.; Srimath, R.; Vignesh, L.; Rajesh, S. Application of Shape Memory Alloys in Engineering—A Review. *J. Phys. Conf. Ser.* **2021**, *2054*, 012078. [CrossRef]
117. Yavuzer, B.; Bicakci, Ü.; Simsek, D.; Ozyurek, D. Effect of Alloying Time and Heat Treatment on Microstructure and Tribological Properties of Mechanical Alloyed CU-AL-NI Shape Memory Alloy. *J. Mater. Eng. Perform.* **2023**, *33*, 11176–11187. [CrossRef]
118. Salwa, P.; Goryczka, T. Crystallization of Mechanically Alloyed NI50TI50 and TI50NI25CU25 Shape Memory Alloys. *J. Mater. Eng. Perform.* **2020**, *29*, 2848–2852. [CrossRef]
119. GöGebakan, M.; Soguksu, A.K.; Uzun, O.; Dogan, A. Production of Cu-Al-Ni Shape Memory Alloys by Mechanical Alloy. In *AIP Conference Proceedings*; American Institute of Physics: College Park, MD, USA, 2007; Volume 899, p. 654. [CrossRef]
120. Lee, T.-J.; Kim, W.-J. Effect of Severe Plastic Deformation and Post-Deformation Heat Treatment on the Microstructure and Superelastic Properties of TI-50.8 at.% Ni Alloy. *Materials* **2022**, *15*, 7822. [CrossRef]
121. Manjunatha, J.G.; Kanthappa, B.; Hareesha, N.; Raril, C.; Tighezza, A.M.; Albaqami, M.D. Enhanced Electrochemical Detection of Rutin Using Poly (Methyl Orange) Modified Carbon Paste Electrode as a Responsive Electrochemical Sensor. *Chem. Afr.* **2023**, *7*, 1141–1150. [CrossRef]

Disclaimer/Publisher's Note: The statements, opinions and data contained in all publications are solely those of the individual author(s) and contributor(s) and not of MDPI and/or the editor(s). MDPI and/or the editor(s) disclaim responsibility for any injury to people or property resulting from any ideas, methods, instructions or products referred to in the content.